



Age Assignment, Palaeoecology and Sequence Stratigraphic Framework of the Nukhul Formation at Wadi Baba, West-Central Sinai (Egypt)

Aziz Abu Shama¹ · Sara El-Nahrawy¹ · Sherif Farouk²

Received: 11 November 2022 / Revised: 26 January 2023 / Accepted: 22 March 2023 / Published online: 2 June 2023
© The Author(s) 2023

Abstract

The Nukhul Formation has been a point of controversy until now due to a lack of index fossils, varied facies modifications, and different time gaps. As a result, the calcareous nannofossils of the exposed Miocene rocks at Wadi Baba, west-central Sinai have been studied quantitatively for the first time. An important sequence of calcareous nannofossil bioevents has been recorded in the Nukhul Formation, including the FOs of *Discoaster druggii*, *Sphenolithus dissimilis*, *Helicosphaera ampilaperta*, and *Sphenolithus disbelemnus*, which correspond to the Aquitanian age of upper NN1 and NN2 zones. The Nukhul Formation contains four intervals that reflect eutrophic conditions in the nearshore habitats with substantial nutrient input from the terrigenous influx, as shown by the dominance of cool-water taxa, *Coccoliths pelagicus* and *Reticulofenestra minuta*. The lithofacies, microfacies types, abundance, dominance, and diversity of nannofossil assemblages classified the studied interval into two depositional sequences with four system tracts. These tracts refer to fluctuations in relative sea level changes in response to the eustatic sea-level curve.

Keywords Calcareous nannofossils · Aquitanian · Burdigalian · Miocene · Rift basin · Sinai · Palaeoecology

Introduction

The Nukhul Formation represented one of the most important oil reservoirs in the Gulf of Suez and west-central Sinai. Several studies have been conducted on the significant Nukhul Formation due to its high-quality oil accumulations (e.g. El Heiny and Martini 1981; Saoudi and Khalil 1986; Evans 1988; El-Azabi 1997, 2004; Phillip et al. 1997; Abul-Nasr and Salama 1999; El-Deeb et al. 2004; Soliman et al. 2012; El Atfy et al. 2013; Temraz and Dypivx 2018; Zalat 2018; Hewaidy et al. 2012, 2014, 2016; Ayyad and Hewaidy 2016). The Nukhul Formation that was deposited above older pre-rift and early rift rock units in marginal marine to shelf environments has a relatively small thickness in outcrops, but borehole data indicate large thicknesses up to 500 m in the West Zeit Trough (Peijs et al. 2012).

The age of the Nukhul Formation in west-central Sinai is still the subject of controversy. Indeed, this formation is considered Aquitanian-early Burdigalian (e.g. Garfunkel and Bartov 1977; El Heiny and Martini 1981, Fawzy and Abdel Aal 1984; Scott and Govean 1985; Evans 1988). It is divided into three time-equivalent members: the Shoab Ali Member and the Ghara, October, and Gharamul Members (Saoudi and Khalil 1986). Dating the Shoab Ali as extending into the late Oligocene based on radiometric data, however, is not confirmed by fossil evidence in the Gulf of Suez and the northern Red Sea (Al-Husseini 2012). However, the palynological study by El-Atfy et al. (2013) suggested the Chattian-Aquitanian age for the Nukhul Formation in some subsurface wells, particularly for Shoab Ali Member. It is worth mentioning that however, they referred to the absence of strong evidence for accurate dating, due to the scarcity of palynomorphs. Moreover, the Nukhul Formation at Wadi Baba (the area of the present study) was dated as late Oligocene-Early Miocene based on planktonic foraminifera and nannofossils (Hewaidy et al. 2012, 2014; Ayyad and Hewaidy 2016). They also mentioned the presence of the Oligocene NP25 Zone of Martini (1971) at the lowermost part of the formation, depending on the presence

✉ Sherif Farouk
geo.sherif@hotmail.com

¹ Department of Geology, Faculty of Science, Kafrelsheikh University, Kafr el-Sheikh 33516, Egypt

² Exploration Department, Egyptian Petroleum Research Institute, Nasr City 11727, Egypt

of *Sphenolithus ciperonsis* in one sample from the base of the section.

The samples for the present work were collected from Wadi Baba for palaeoecological and palaeoenvironmental studies, as well as for the sequence stratigraphy of the Nukhul Formation deposits. Careful and frequent examination of all samples revealed the absence of calcareous nanofossil bioevents and evidence of the late Oligocene in the Nukhul Formation. The aims of this study are to revise and introduce the age assignment and palaeoecological implications of the Nukhul Formation at Wadi Baba based on quantitative calcareous nanofossil biostratigraphic studies, in addition to the sea level response on vertical facies changes and palaeo-productivity.

Geologic setting and general lithostratigraphy

The Gulf of Suez is a rift graben between the two uplifts of the Sinai and the Eastern Desert (Schütz 1994). The movement of the Nubian and Arabian shields, as well as the Sinai microplate, caused complex faulted and fractured areas in this area. The age of the rift ranges from 23 to 27 Ma (Bosworth and McClay 2001). The initiation of the rift system is assigned to the latest Oligocene-earliest Miocene age (e.g. Garfunkel and Bartov 1977; Moustafa 1993; Patton et al. 1994). The stratigraphic section of the Gulf of Suez and the northern Red Sea deposits are subdivided into pre-rift and syn-rift deposits (Robson 1971; Moustafa 1987; Sharp et al. 2000; Jackson et al. 2006). According to Moustafa and Khalil (2020), a third division, post-rift rocks exist only in the Suez Rift, whereas the Red Sea is still extending. The pre-rift rocks of the Gulf of Suez and the northern Red Sea include platform sedimentary units unconformably overlying the Precambrian crystalline basement rocks. The pre-rift deposits are unconformably overlain by the Oligocene-Miocene syn-rift succession (Garfunkel and Bartov 1977; Patton et al. 1994). The syn-rift sequence includes an early rift sequence (red beds and Abu Zenima Formation) unconformably overlain by proper syn-rift sequences (Moustafa and Khalil 2020). The proper syn-rift sequence is represented by the Miocene sediments.

There are many attempts to study and classify the Miocene succession in the Gulf of Suez and western Sinai (e.g. EGPC 1964; NSSC 1974; Saoudi and Khalil 1986). The Miocene succession is divided into two major groups: the Lower Miocene Gharandal group, which includes the Nukhul, Rudies, and Kareem formations, and the Upper–Middle Miocene Ras Malaab group, which includes the Belayim, South Gharib, and Zeit formations (El-Ayouty 1990; Hughes et al. 1992). In the Aquitanian, deposition of the proper syn-rift sediments started with a phase of slow tectonic subsidence followed by a phase of rapid subsidence at ~20 Ma. This phase was

followed at ~17 Ma by another phase of slow tectonic subsidence (Moustafa and Khalil 2020). This tectonic activity resulted in the erosion of the structurally high Nukhul sediments, and the subsidence of the rift led to the deposition of the Burdigalian Rudies Formation (Moustafa 1993).

The Nukhul type section is located in Wadi Nukhul in the west-central Sinai Peninsula (29° 01' 30" N; 33° 11' 30" E) and is 74 m thick. It was first named by Waite and Pooley (1953) and then formally established by the EGPC (1964). This formation was deposited while the water depth in the Gulf of Suez was shallow and sedimentation occurred through rapid subsidence (Saoudi and Khalil 1986). The rifting led to changes in lateral and vertical facies from continental deposits to a marginal marine succession of the Nukhul Formation (Patton et al. 1994). The degree of erosion and uplift varies in the area, so the Nukhul Formation overlies rocks ranging from Pre-Cambrian to middle Eocene ages, depending on the degree of erosion in the area (Richardson and Arthur 1988). The Nukhul Formation is underlain by the Abu Zenima Formation, which accumulated during the early stages of rifting in the northern and central parts of the Gulf of Suez. Generally, deposits of the Nukhul Formation are related to offshore, shoreface, and estuarine settings (Carr et al. 2003; Gadallah et al. 2007). The Nukhul Formation in the studied area unconformably overlies the middle Eocene Darat Formation, separated by a 5 m thick conglomeratic layer with large boulders, fossil fragments, and a calcareous matrix. It underlies unconformably the Rudies Formation, where the vertical facies changes from being dominated by burrowed calcareous sandy content to marl and argillaceous limestone.

Tectonically, the Gulf of Suez rift was divided into three 50–100 km-long tectonic domains (Colletta et al. 1988; Patton et al. 1994; Moustafa 1996): (1) the northern Darag basin; (2) the central basin; and (3) the southern basin. Two major wide accommodation zones exist in between (Colletta et al. 1988): the Zaaфарana and the Morgan accommodation zones. The facies distribution of the Nukhul Formation was influenced by large-scale tectonics (e.g. accommodation zones, Darag, Central, and Southern basins) as well as small-scale structures (Rohais et al. 2016). The Nukhul Formation is subdivided into two members: Shoab Ali and laterally time equivalent members (Ghara, October, and Gharamul) (Saoudi and Khalil 1986). The Shoab Ali member is composed of continental deposits and is concentrated in the rift's southern areas (Patton et al. 1994). The Ghara member was originally described by Saoudi and Khalil (1986). It is composed of white, hard anhydrite layers interbedded with sandstones, grey marls, calcareous shales, and limestones. Palaeogeographically, three key phases (Nu1–Nu3) during the Nukhul Formation deposition were established by Rohais et al. (2016), in which the time frame defined by Hughes et al. (1992) was used. During the first phase (20.4–23

Ma), the southern basin was composed of siliciclastic deposits, the Morgan accommodation zone was sub-aerial, and the central basins (e.g. the Baba area) were characterised by shallow marine to a restricted setting. The transition from shallow marine to open marine settings was in Zaafarana and Darag, respectively. In the second phase (21.2–22.1 Ma), marine flooding from the Mediterranean invades from the north to the central basin, and carbonates and deep marine shale are deposited. The lagoon and Sabkha evaporites characterised the southern basin at this stage. In the last phase (20.4–21.2 Ma), the marine flooding from the Mediterranean reaches the Morgan accommodation zone, and the input of terrigenous deposits becomes localised to the rift shoulders. The southern basins were characterised by isolated evaporite ponds (see maps in Popov et al. 2004; Rohais et al. 2016).

Material and Methods

Eighty-seven samples, with 30–100 cm spacing between samples, were obtained from the exposures of Wadi Baba, east of Abu Zenima locate at 33°15'784"E and 28°57'270"N (Fig. 1). The samples were prepared using standard nannofossil smear slide techniques, as described by Perch-Nielsen (1985) and Bown and Young (1998). The studied nannofossil assemblages were investigated under 1000X magnification with cross-polarized light using an Olympus TH4-200 microscope equipped with Olympus UC-30 camera. The zonal scheme for this study follows the nannoplankton zonation schemes of Okada and Bukry (1980), Martini (1971), and Backman et al. (2012). Preparing the samples for the quantitative analysis, the settling technique of Geisen et al. (1999) are used. The qualitative and quantitative nannofossil

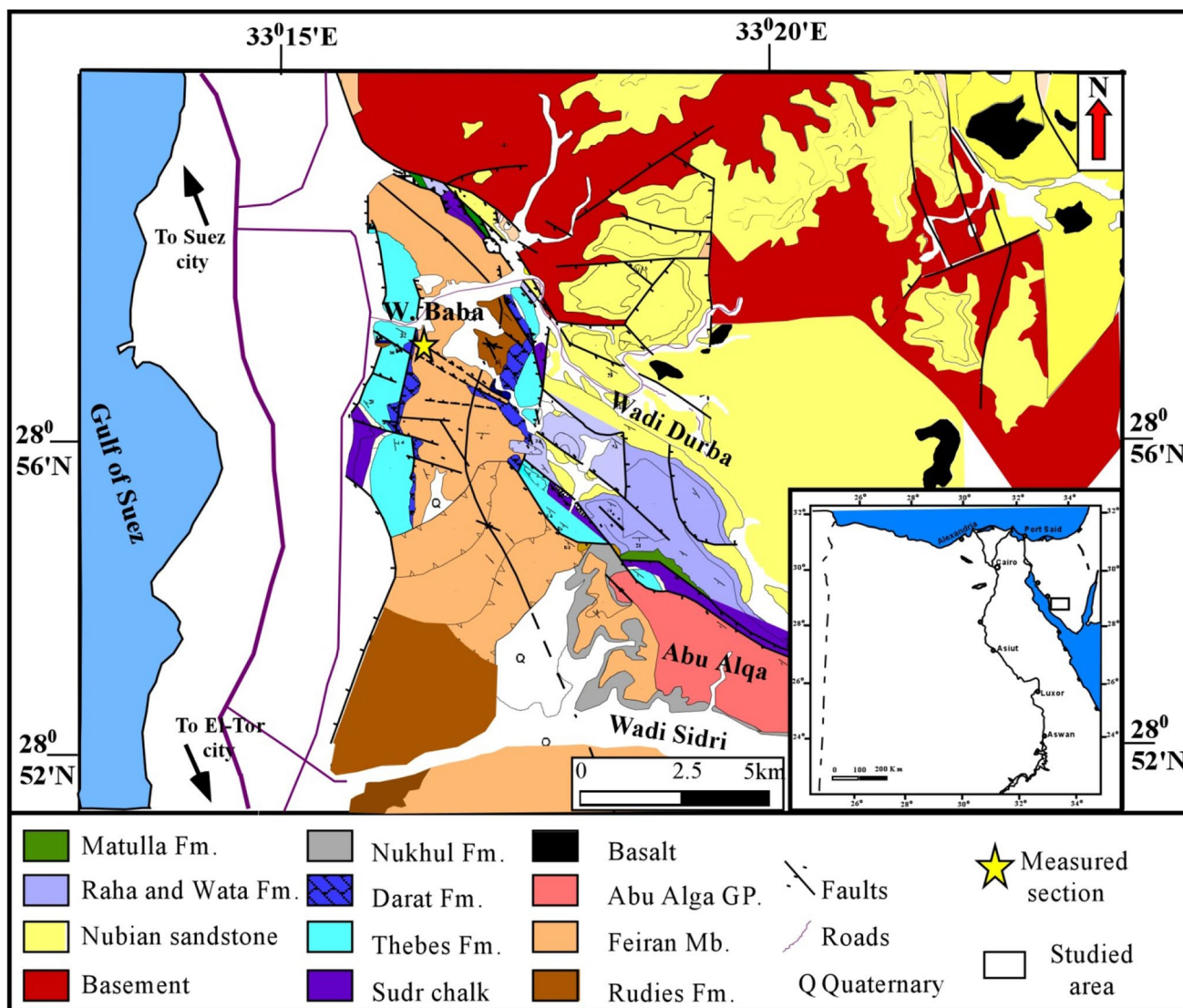


Fig. 1 The geologic map (modified after Moustafa 2004) of the studied section (Wadi Baba) in west-central Sinai (Egypt)

taxa are accomplished by counting around 100 to 300 individuals, with the exception of some samples that contain low-abundance individuals. PAST software was used to group the samples into clusters and describe the palaeo-productivity based on diversity indices including species richness, the dominance index, and the Shannon-Weiner diversity index (Hammer et al. 2001; Hammer and Harper 2006; Wade and Bown 2006). Twenty microfacies thin sections were prepared and classified according to Dunham (1962) for the carbonate rocks, whereas the sandstone was classified according to Pettijohn et al. (2012).

The samples are deposited in the Paleontology and Sedimentology Laboratory, Geology Department, Faculty of Science, Kafrelsheikh University, Egypt.

Results

Lithofacies and microfacies types

A detailed field and petrographical description identified the following five lithofacies and microfacies types:

Conglomerates (LFt-1)

This lithofacies occurs unconformably at the contact between the middle Eocene Darat Formation and the Lower Miocene Nukhul Formation (bounded at the base by an erosional surface) with a thickness of 5 m (Figs. 2a; 3). The clasts are medium to highly rounded, with sizes ranging from 5 to 100 mm. The pebbles and gravels are floated in a matrix of coarse sand and lime muds and are composed mainly of white limestone and chert fragments, but rarely mudstone. This lithofacies is poorly sorted, polymictic, unstratified and contains reworked fossil fragments. The texture of this type of lithofacies is immature, massive and contains different types of materials with varying sizes of grain. As a result, the conglomerates form channels that fill debris flow in alluvial fans (Blair and McPherson 1994). Such massive clast-supported conglomerates are interpreted as a result of debris flow deposits and are considered as channel lag sheets or channel bars (e.g. Lowe 1982; Nemeč and Steel 1984; Postma 1984; Mulder and Alexander 2001).

Cross-bedded sandstone (LFt-2)

This type of lithofacies is concentrated in the lower part of the Nukhul Formation (Fig. 3). Cross-bedding is the main sedimentary structure characterising this facies. The main sedimentary structure of this lithofacies is planar cross-bedded. The grains are medium to coarse sand with sizes up to 1 mm. The thickness of sandstone beds varies from 0.5 m to 2.5 m and is rich in pecten and oysters. The

cross-bedded sandstone lithofacies contains scattered pebble size black chert grains (Fig. 2b). Massive sandstone is rarely found in the studied Nukhul Formation and often presents in the base of small fining upward cycle along with sandy limestone lithofacies. The microfacies type of this lithofacies is a calcareous bioclastic sublithic arenite (MF1). This microfacies is poor to moderately sorted sandstone with associated fossil fragments. The facies is mostly made up of subangular to subrounded detrital quartz (40 to 55 %). The quartz grains are monocrystalline, rarely polycrystalline, and fine to coarse in size. Calcite and iron oxides are common in the sandstone. Quartz grains are frequently corroded and replaced by calcite. Some feldspars grains were replaced by calcite. This is evidenced by the very rare remnants of visible feldspars. The associated bioclastic grains represent 5 to 15% of the total rock. The framework grains are embedded in sparry poikilotopic calcite cement.

At the lowermost part of the Nukhul Formation, the calcareous sublithic arenite has reworked planktonic foraminifera and little benthic foraminifera (samples B4, B6, and B7) (F. 4a). In the next samples of the Nukhul Formation (samples B9 and B10), the associated bioclasts with detrital quartz are oyster shell fragments, little planktonic foraminifera, brachiopods, and echinoderm spines (Fig. 4b). The oyster shell fragments are partially altered by silicification. Rounded to angular, and medium to coarse in size glauconite grains constitute about 2 to 5%. Other lithic fragments are recognised, such as angular to subangular black chert fragments, as well as spherical disoriented brown lithic fragments and disoriented phosphatic grains.

At the middle part of the Nukhul Formation, the grains of this microfacies are cemented with ferroan sparry calcite with some scattered micrite matrix and iron oxides. This facies also contains large rounded and brown lithic fragments as well as calcite fragments. The bioclast fragments are rare (5%) and include molluscan shell fragments, algae and rare ooids. Siliciclastic materials are generally accumulated close to the shoreline, which is supported by the associations of bioclast fragments. The high quartz grains with marine conditions indicate proximity to the shoreline and suggest tidal flats (Flügel 2004).

Sandy limestone (LFt-3)

This lithofacies unit is well distributed in the studied section and varies in thickness from 1 to 2 m. Cross-bedding is the main sedimentary structure in this facies. It has yellowish white and white colours, and fossiliferous with pecten and oysters (Fig. 2c-2e). It is characterised by disseminated and scattered pebble-sized grains and bioturbated at the contact with overlying Rudies Formation (Fig. 2f). The microfacies types are the following:

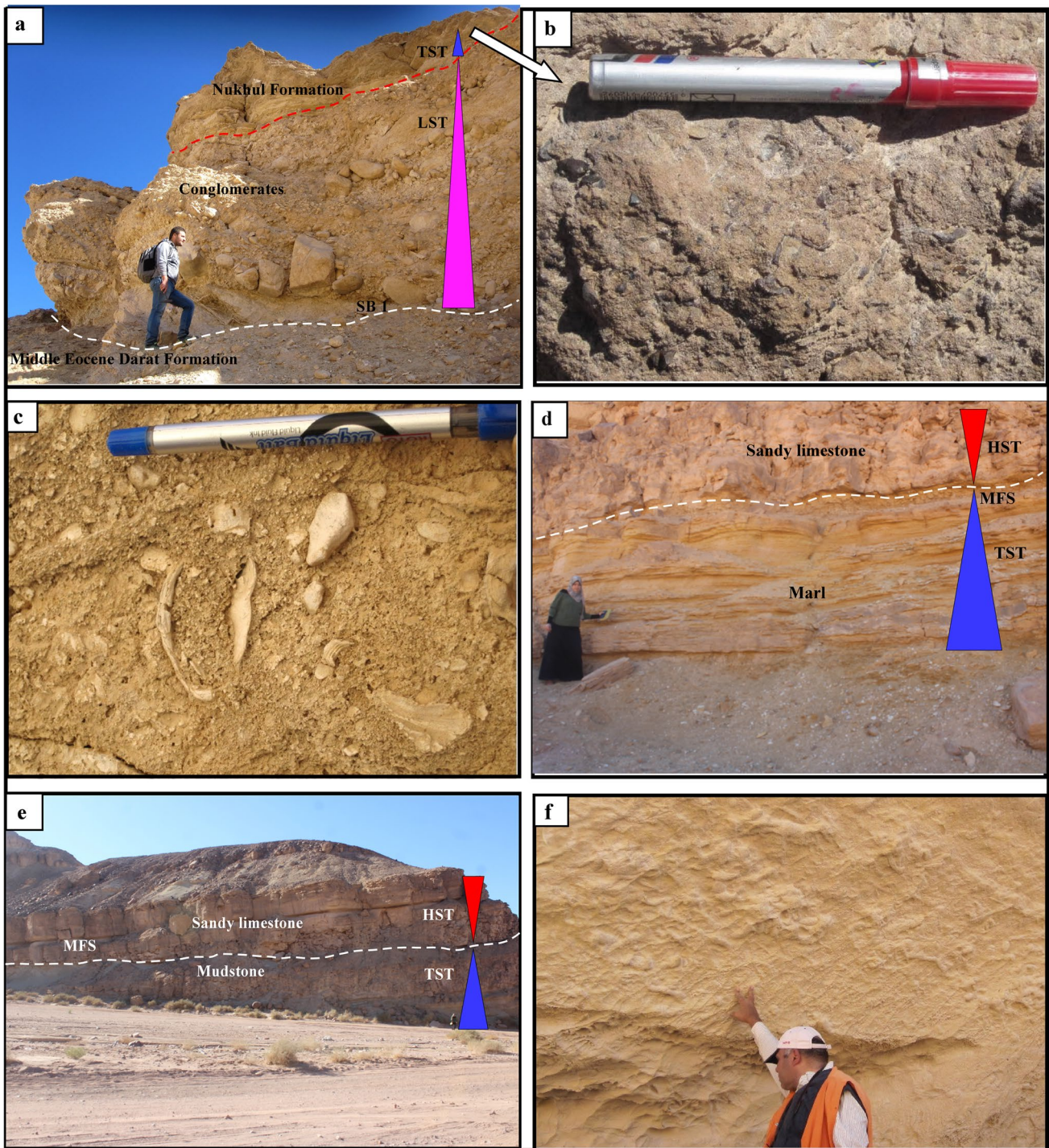


Fig. 2 Field photographs of the studied Nukhul Formation at Wadi Baba **a** The contact between the Nukhul Formation and the underlying middle Eocene Darat Formation. The two formations are separated by a polymitic conglomerate layer. **b** Sandstone lithofacies unit overlies the conglomerate layer at the lowest part of the Nukhul Formation. **c** The sandy limestone lithofacies unit with oyster and pecten.

d Marl is intercalated with thin layers of fossiliferous sandy limestone representing the TST, and overlying sandy limestone and sandstone layers representing the HST. **e** Maximum flooding surface separates the mudstone unit from the sandy limestone unit. **f** the uppermost part of the Nukhul Formation is characterised by a burrowing sandy limestone unit

Microfacies MF2- Packed sandy oyster rudstone: The characteristic feature of microfacies MF2 is a grain-supported texture with abundant bioclasts in a blocky and drusy sparry calcite and in other parts of a micritic groundmass. The microfacies include coarse-grained bioclasts of oysters (Fig. 4c) which are larger than 2 mm in size (30%) and shell fragments of other bivalves (25%). The framework grains are well-oriented. Some oyster shell fragments are exposed partially to micritization. The effect of compaction and the formation of void-filling spars are also observed. At the lower part of the Nukhul Formation (samples B8, B17, and B18), the sandy limestone unit encompasses a high percentage of quartz grains, and the grains are oriented and laminated. The laminae are alternations of quartz grains cemented by calcite, and packed oysters and other bioclasts in micro- and pseudo-sparite. Oysters occur at a depth of less than 50 m in low-oxygenated and nutrient-rich waters (Gertsch et al. 2010). The variety in quartz grain sizes from fine to coarse is an indicator for mixing from different depositional environments or multiple sources (Scholle and Ulmer-Scholle 2003). Therefore, the occurrence of shallow marine fauna with sparry cement and a high percentage of quartz grains indicate tidal flat or shoal deposition leeward where the bioclasts have been mixed during the storm (Flügel and Munnecke 2010).

Microfacies MF3- Sandy bivalve grainstone-rudstone: This microfacies is well encountered in the middle parts of the Nukhul Formation within samples B36 and B39. The main framework grains are bivalves (Fig. 4h) which form about 45% of the total volume of the rock and oysters of about 10%. The other bioclast fragments are intraclasts, bryozoa, echinoids, miliolids, and small shell debris. Quartz and black chert fragments are the associated clastic grains. The quartz grains are medium to very coarse, subrounded to angular, and monocrystalline. Echinoderms and bivalves refer to high-energy, open circulation, and normal salinity environments above the fair-weather wave base (Wilson 1975). The presence of intraclasts with sparry calcite is indicative of high energy conditions (Flügel and Munnecke 2010). The presence of sparite cement indicates the deposition of erosive tidal channels of barriers in high energy environments (Tucker and Wright 2009) that connect at lagoonal with the open marine environment. In summary, these microfacies indicate a shoal or open marine setting.

4Microfacies MF4- Recrystallised bioclastic grainstone: It is recognised in the latest samples of the Nukhul Formation. It contains foraminifera, molluscan shell fragments, and calcareous algae embedded in a groundmass made of blocky and drusy sparry calcite cement. The framework grains as well as the groundmass are exposed to intensive

recrystallization with sparry calcite. Little scattered terrigenous quartz grains are also found in this microfacies. The drusy calcite cement is commonly observed and it can be interpreted as deposits of late diagenetic processes (Flügel 2010). This process is attributed to the meteoric influence as a result of sea level falling (Scholle and Ulmer-Scholle 2003).

Microfacies MF5- Sandy bioclastic packstone: It contains framework grains embedded in micrite matrix (packstone). The main allochems are benthic foraminifera with spar-filled chambers (20%, mainly *Nummulites* sp. and other types), oyster shell fragments (15 to 20%) and intraclasts (approximately 10%; Fig. 4f, g). Most of the intraclasts are well-rounded to subrounded; and polymodal in size. The intraclasts are composed of different forms of fossil shell fragments and others from planktonic foraminifera. Secondary bioclasts are mainly corals, echinoids, bryozoans, red algae, and fragments of mollusks. In this microfacies, some voids are filled with chalcedony; and the oyster shells are partially micritized and/or silicified. The detrital quartz grains are coarse to medium, poorly sorted, angular to subrounded monocrystalline quartz (approximately 30%). The packstone-grainstone is poorly-medium sorted and the grains are angular to subangular. The *Nummulites*, bryozoans, and echinoids are open marine skeletal fauna (Hottinger 1983, 1997; Romero et al. 2002). Bivalves, bryozoans, and echinoids indicate a high-energy lagoonal setting above fair-weather wave base (Wilson 1975). *Nummulites* can be considered as a proxy for deposition in open marine and inner ramp settings (Adabi et al. 2008). This microfacies is deposited in a medium-energy open marine environment. Accordingly, this microfacies may belong to FZ 7-8 of Wilson (1975) and was accumulated in an outer lagoon/open marine setting.

Microfacies MF6- Foraminiferal pack-grainstone: It is detected at the lowermost part of the Rudies Formation. It contains planktonic and small benthic foraminiferal tests embedded in sparite and micritic matrix (Fig. 4i). The percentage of planktonic to benthic foraminifera is approximately 55 to 60%. Benthic foraminifera are composed of small uniserial and biserial tests. The planktonic foraminifera are unkeeled tests. The presence of planktonic foraminifera indicates an open, deep marine setting below the photic zone (Geel 2000). Bassiouni and Luger (1990) reported that the outer ramp setting is distinguished by a planktonic/benthic (P/B) ratio of more than 61%, and the middle ramp environment has a P/B ratio ranging from 25 to 41%, referring to deposition in the middle/outer ramp setting. The presence of micrite as well as sparite indicates moderate-energy.

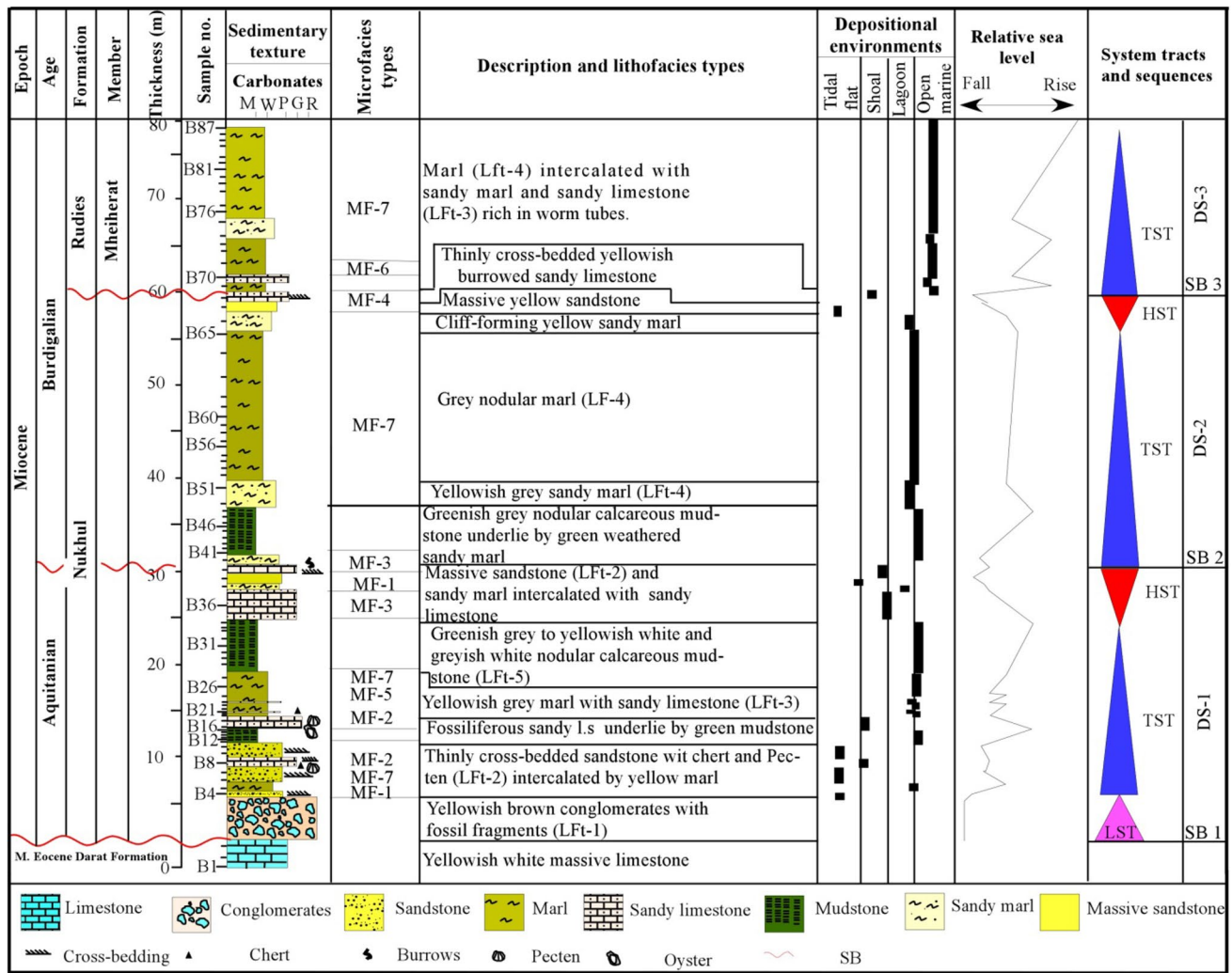


Fig. 3 Lithostratigraphic column, microfacies types, depositional environment, system tracts, sea level curves, and depositional sequences of the Miocene Nukhul Formation and the lowermost part of the Rudies Formation at Wadi Baba, west-central Sinai (Egypt)

Marl and sandy marl lithofacies (LFt-4)

The marl and sandy marl lithofacies are two of the most abundant lithofacies in the studied rocks (Fig. 2d). The unit is flaky and nodular marl and sandy marl, varying in colour from grey to yellow, light green, and yellowish grey. It occurs in fine upward cycles, mainly overlain by sandy limestone and sandstone lithofacies. The marl and sandy marl lithofacies are mainly fossiliferous in the lower and upper parts of the section and lack fossils in the middle part of the Nukhul Formation. The recorded microfacies are sandy benthic foraminiferal wacke-mudstone and planktonic/benthic foraminiferal wacke-mudstone.

Microfacies MF7- Sandy foraminiferal wacke-mudstone: This microfacies is well encountered in the studied section. In the Nukhul Formation, it contains small benthic foraminiferal

tests (10 to 15%) embedded in the micrite matrix (about 60 to 70%; Fig. 4d, e). The microfacies contains randomly disseminated fine to medium; subrounded to subangular quartz grains. Besides the foraminiferal tests, the allochems include rare echinoid and bivalve fragments in some samples. It is noted that this microfacies in the marl of the lower part of the Rudies Formation contains unkeeled planktonic foraminiferal tests as well as small benthic foraminifera embedded in an approximately 70 to 90% lime-mud matrix. This microfacies is deposited in an open lagoon above a fair-weather wave base of the normal marine setting (FZ 7 of Wilson 1975; Flügel 2010). The dominance of the micritic matrix suggests a low-energy environment below the storm wave base (Burchette and Wright 1992). The P/B ratio of 1 to 5% indicates an inner shelf setting and the presence of planktonic foraminifera indicates a deep outer shelf marine setting (Geel 2000; Romero et al. 2002; Pomar et al. 2014).

Calcareous mudstone lithofacies (LFt-5)

Fine-grained mud rocks are concentrated in the lower and middle parts of the studied section and often overly the marl lithofacies (Fig. 2e). This lithofacies is observed in grey, yellowish grey and green colours. Although the grain sizes are mostly clay and silt, they partly exhibit fine sand sizes. The main observed sedimentary structure is horizontal laminations. The micritic matrix indicates a low-energy depositional environment in open marine and normal salinity conditions (Wilson 1975; Flügel 2010). This lithofacies is highly fossiliferous with nannofossils and indicates a middle/outer ramp setting.

Biostratigraphy

Three biozones were identified based on the vertical distribution of the first occurrence (FO) and last occurrence (LO) of the calcareous nannofossil marker species (Figs. 5–6). Below is a brief summary of each recorded zone, from oldest to youngest.

The NNI Zone of Bramlette and Wilcoxon (1967) emended by Martini and Worsley (1970)

This zone can be detected from the LOs of *Helicosphaera recta* or *Sphenolithus ciperonesis* to the FO of *Discoaster druggii*. A major hiatus between the middle Eocene Darat

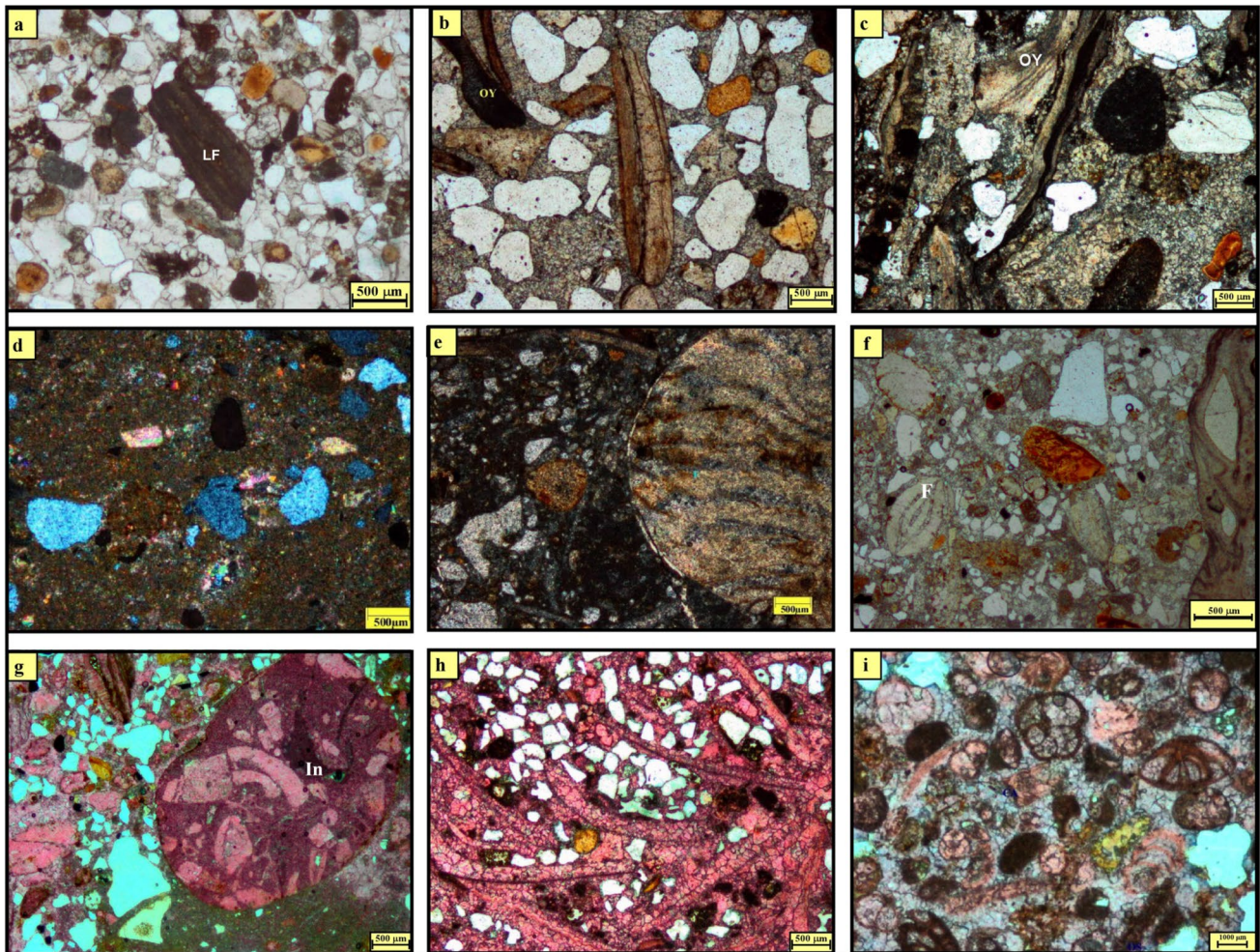


Fig. 4 Photomicrographs from the detected microfacies associations of the Nukhul Formation in the studied section (a–h) and of the Rudies Formation (i); a–f unstained thin sections; g, h, i stained thin sections. a–c, e–g plain polarized light and d, h, i crossed nicols, a Sublithic calcareous bioclast arenite (LF), reworked planktonic foraminifera and glauconite (MF-1). b Oyster (OY), shell fragments,

planktonic foraminifera, and glauconite sublithic calcareous bioclast arenite (MF-1). c Sandy oyster rudstone (MF-2) microfacies. d, e Sandy lime-mudstone microfacies (MF-7). f, g Benthic foraminifera (F) and intraclasts (In) in a sandy bioclast packstone (MF-5). h Sandy bivalve grainstone-rudstone (MF-3). i Foraminiferal pack-grainstone microfacies (MF-6)

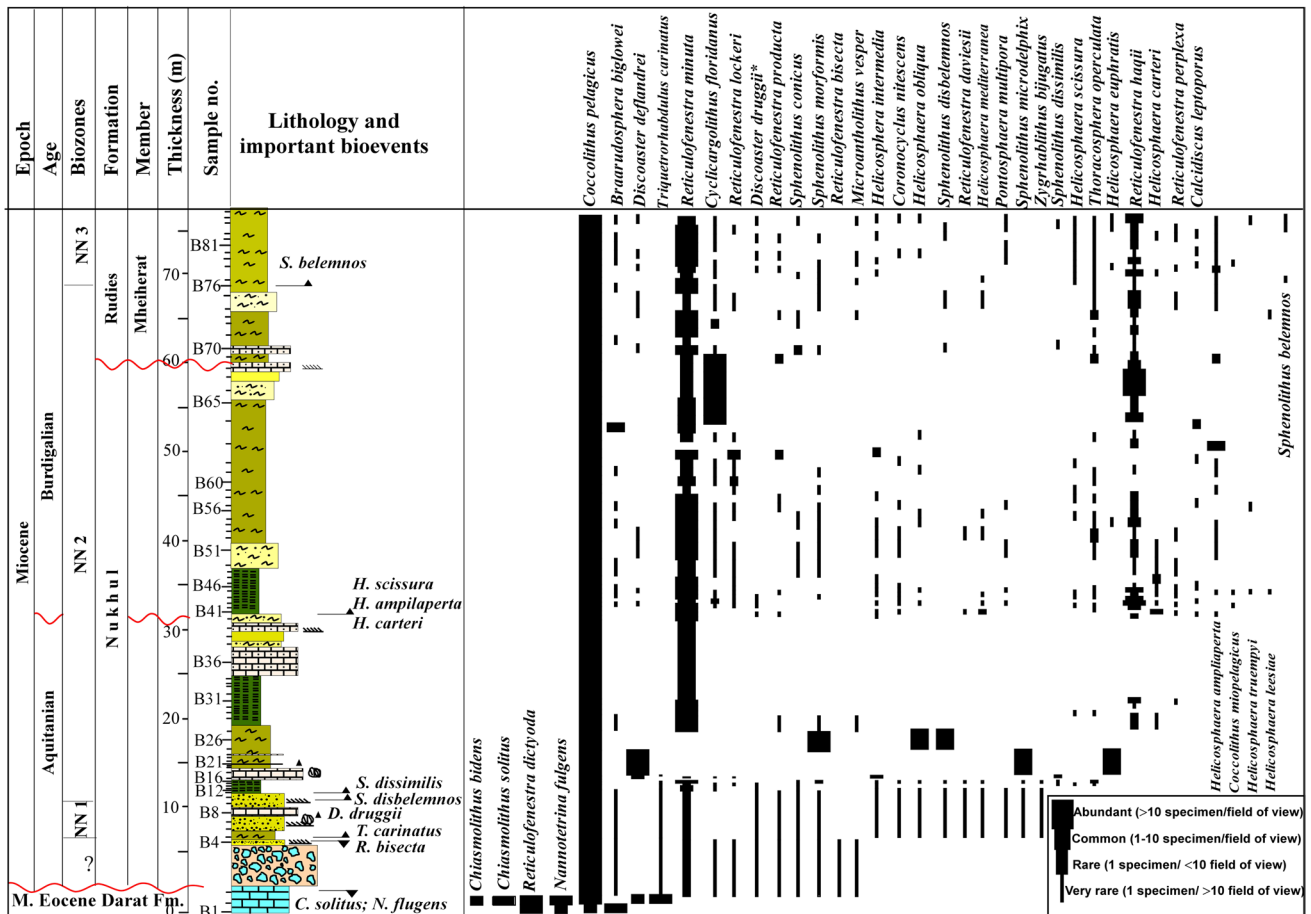


Fig. 5 Distribution chart of the calcareous nannofossil species recorded in the Wadi Baba section

Formation and the overlying Nukhul Formation where the NN1 overlies the middle Eocene calcareous nannofossil Zone NP15, which is defined by the FO of *Nannotetrina fulgens* to the FO of *R. umbilica* (samples B1–B3). The NN1 Zone of Martini (1971) is equivalent to CN1b of Okada and Burky (1980) and corresponds to CNM1 of Backman et al. (2012) (Fig. 7). The thickness of this zone attains about 5 m and it is represented by samples B4–B10. Except for sample B5, this interval is barren of nannofossils (Fig. 3). The most common nannofossil assemblages are *Coccolithus pelagicus*, *Reticulofenestra bisecta*, *Triquetrorhabdulus carinatus*, *Cyclicragolithus floridanus*, *Braarudosphaera bigelowii*, *Sphenolithus conicus*, *Helicosphaera intermedia*, *H. mediterranea*, *Sphenolithus moriformis*, *Discoaster deflanderi*, and *D. druggii* of size less than 10 µm.

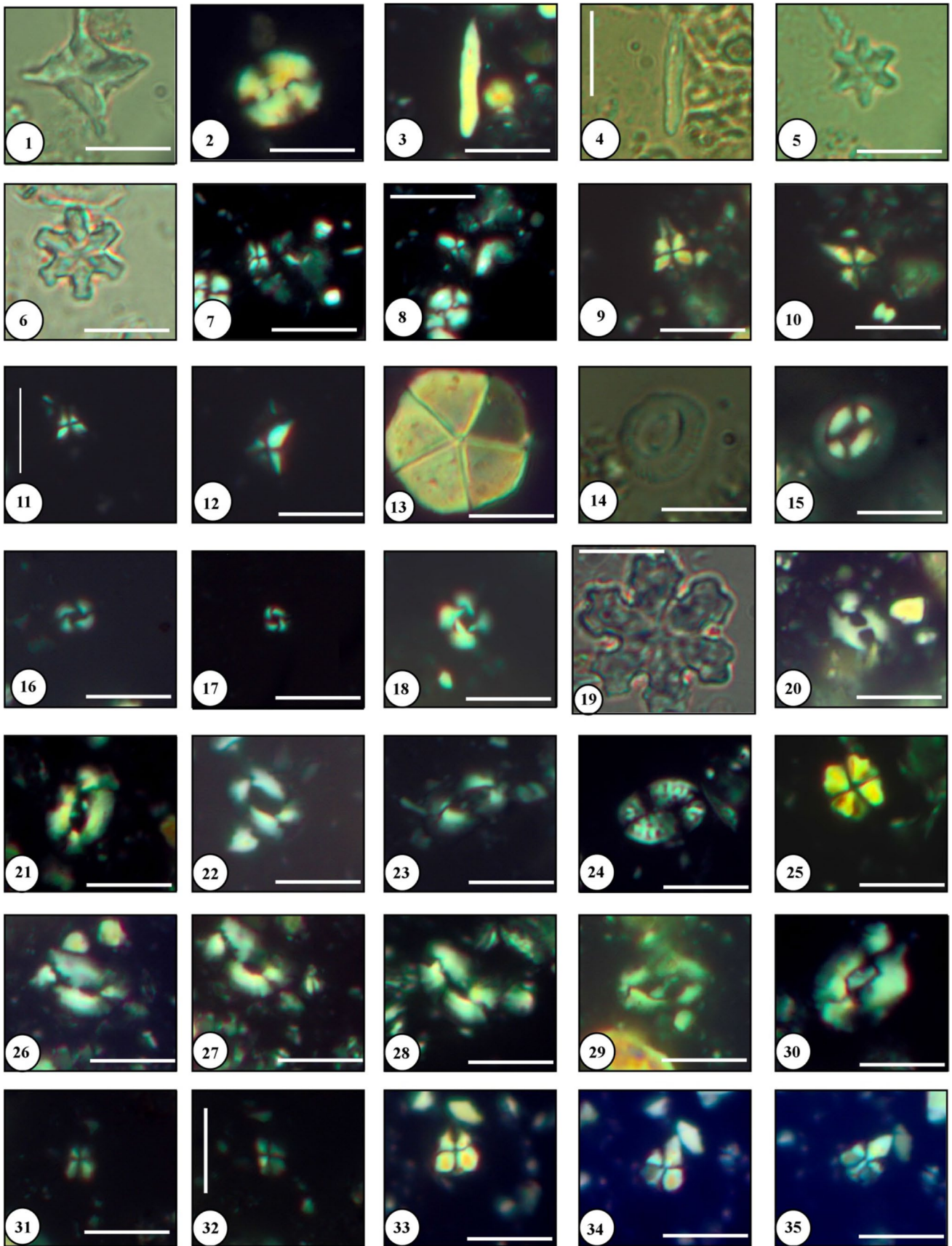
The NN2 Zone of Martini and Worsley (1970)

It is defined from the FO of *Discoaster druggii* to the LO of *Triquetrorhabdulus carinatus*. The thickness of this zone is about 55 m and it is represented by samples B11 to B75. It can

be subdivided into lower and upper NN2 zones, marked and separated by the FO of *H. ampliperta* (Raffi et al. 2006). The lower part of the NN2 Zone (samples B11 to B40) is equivalent to the CNM2 Zone of Backman et al. (2012) (Fig. 7). The lower interval is characterised by the same assemblage of the NN1 Zone besides the occurrence of *S. microdelphix*, *S. disbelemnus*, *S. dissimilis*, and *D. druggii* with a size of 10–15 µm. The upper part of the NN2 Zone is recorded within samples B41 to B71 and is equivalent to the CN1c *Discoaster druggii* Subzone of Okada and Bukry (1980). It corresponds to the CNM4 nannofossil zone of Backman et al. (2012). *C. pelagicus*, *C. floridanus*, *Reticulofenestra haqii*, and *R. minuta* are abundant in this interval. This part contains less abundant specimens of *Helicosphaera carteri*, *S. dissmillilis*, *S. moriformis*, *D. deflandrei*, *H. intermedia*, *H. ampliperta*, *H. scissura*, *B. bigelowii*, *S. disbelemnus*, and *S. conicus*.

The NN3 Zone of Bramlette and Wilcoxon (1967) emended by Martini (1971)

This zone covers the interval from the LO of *Triquetrorhabdulus carinatus* to the FO of *Sphenolithus belemnus*. The



◀**Fig. 6** The bar scale = 10 μm. **1** *Nannotetrina flugens*, Sample B1. **2** *Reticulofenestra bisecta* Sample B5. **3** (XP), **4** (PL) - *Triquetrorhabdulus carinatus*, Sample B11. **5, 6**- *Discoaster druggii*. **5** Sample B 11, **6** Sample B74. **7, 8** *Sphenolithus dissimilis*, Sample B12. **9, 10** *Sphenolithus conicus*, Sample B11. **11, 12** *Sphenolithus microdelphix*, sample B11. **13** *Braarudosphaera bigelowii*, Sample B11. **14** (PL), **15** (XP) - *Coccolithus pelagicus*, Sample B27. **16** *Reticulofenestra haqii*, Sample B60. **17** *Reticulofenestra minuta*, Sample B80. **18** *Cyclicargolithus floridanus*. Sample B37. **19** *Discoaster deflandrei*, Sample B70. **20** *Helicosphaera mediterranea*, Sample B47. **21, 22** *Helicosphaera ampliapertura*. **21** Sample B75, **22** Sample B79. **23** *Helicosphaera scissura*, Sample B72. **24** *Pontosphaera multipora*, Sample B44. **25** *Sphenolithus moriformis*, Sample B11. **26, 27, 28** *Helicosphaera carteri*, Sample B40. **29, 30** *Helicosphaera intermedia*. **29** Sample B 11, **30** Sample B 72. **31, 32** *Sphenolithus disbelemnus*. Sample B79. **33, 34, 35** *Sphenolithus belemnus* (Sample B80)

NN3 Zone is recorded from the base of Rudies Formation (samples B76 to B87) and attains a thickness of about 7 m. It correlates with the CN2 *Sphenolithus belemnus* Zone of Okada and Bukry (1980). It corresponds to the CNM5 Zone of Backman et al. (2012) (Fig. 7). Abundant occurrences of *C. pelagicus*, *C. floridanus*, and *R. minuta* were recorded in this interval. *Discoaster druggii*, *H. mediterranea*, and *S. moriformis* are also recorded in this zone.

Nannofossil abundance and assemblages

Based on the R-mode cluster analysis (Fig. 8), three groups are identified

Group A

It includes both *C. pelagicus* and *R. minuta*. The *C. pelagicus* appears continuously and is the most abundant in the investigated samples, reaching an amount of up to 83% in some samples. *R. minuta* is a major component of the assemblage and its abundance values range from 53% to 6%. Both *C. pelagicus* and *R. minuta* show the highest abundance in the lowermost part of the NN2 Zone and the lower part of the NN3 Zone.

Group B

It corresponds to all the warm taxa whose abundance is less than 4%. These taxa include all the species of *Discoaster*, *Sphenolithus*, *Pontosphaera*, *Brarrudosphaera*, *Micrantholithus*, and *Helicosphaera*. *Sphenolithus moriformis* is the most abundant species in the *Sphenolithus* group. Discoasters show major types of 5-ray and 6-ray types.

Age (Ma)	Epoch	Stage	Standard global zonation			Present study	
			Okada and Burky (1980)	Martini (1971)	Backman et al. (2012)		
17	Miocene	Burdigalian	CN3	NN4	CNM6	<i>S. heteromorphus</i> BZ	out of the study
18			CN2		CNM5	<i>S. belemnus</i> BZ	
19			CN1C	NN2	CNM4	<i>H. carteri</i> PRZ	Not detected
20					CNM3	<i>H. euphratis</i> PRZ	
21	Oligo.	Aquitainian	CN1b	NN1	CNM2	<i>S. disbelemnus/T. carinatus</i> CRZ	Not detected
22					CNM1	<i>S. conicus</i> PRZ	
23			Chatthian	CN1a	NP 25	CNO6	<i>T. carinatus</i> PRZ
24							

Fig. 7 Correlation of the Miocene zonations of Martini (1971), Okada and Bukry (1980), Backman et al. (2012) and the current study

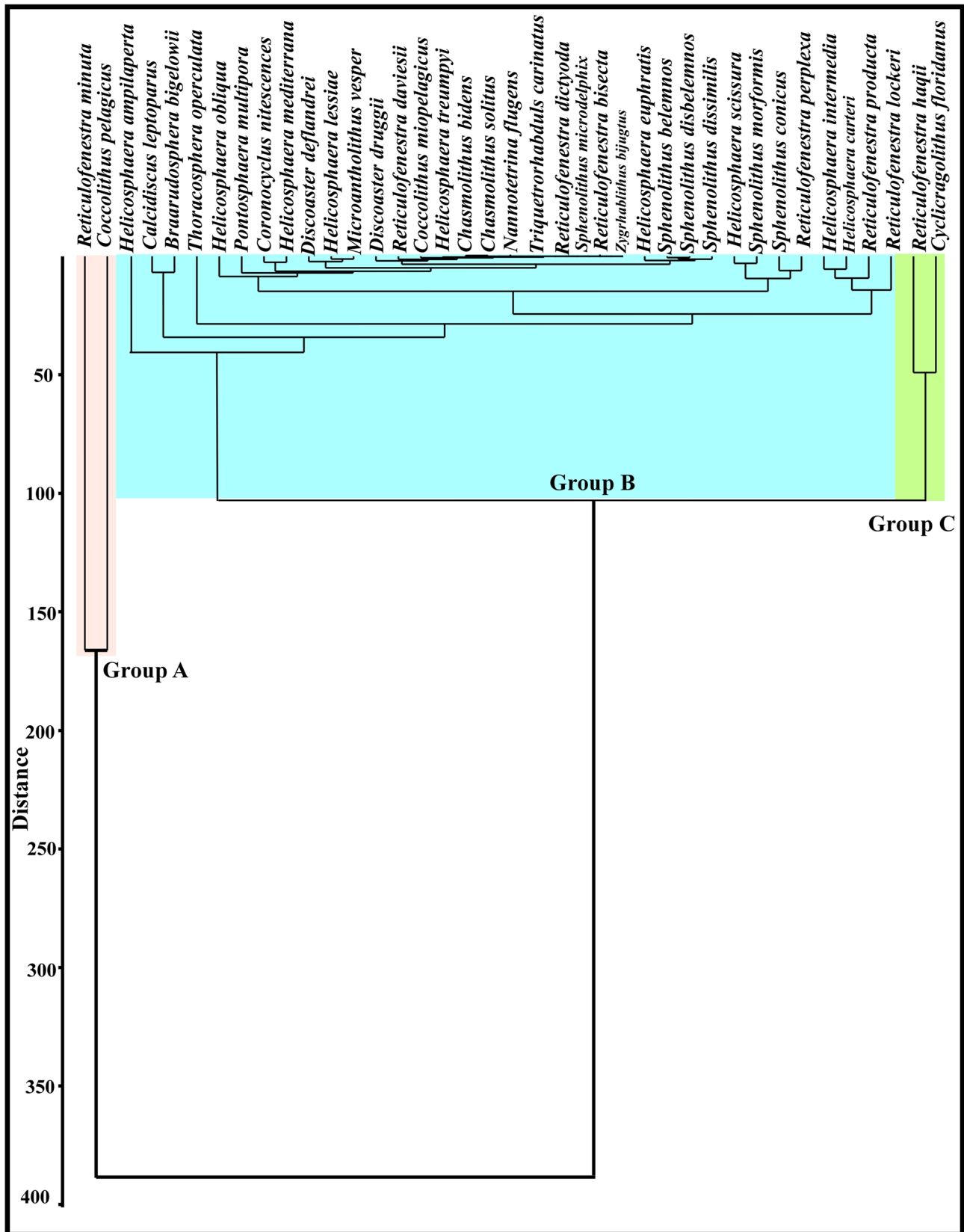


Fig. 8 Multivariate clustering analysis of the studied section transformed abundances of the recorded taxa using Ward's method. The similar coloured lines represent taxa with the same palaeoecological preferences

The majority of *Helicosphaera* types which are recorded in the studied section are *Helicosphaera intermedia*, *H. mediterranea*, *H. euphratis*, *H. carteri*, and *H. ampilaperta*, which are only recorded in the upper part of the section. *Triquetrohabdulus carinatus* is rare and appears in a few samples of the NN1 Zone.

Group C

It includes *C. floridanus* and *R. haqii*. The abundance of *R. haqii* reach about 29% and their increase in abundance occurs in the middle part of the NN2 Zone at the base of Aquitanian than in its upper part. *C. floridanus* is highly variable in the studied section and ranges in abundance from less than 1% to 38%. It has a sharp increase in samples from B64 to B68 in the middle-upper part of the NN2 Zone.

Nannoplankton species richness and diversity

Three taxa were common throughout the assemblages, forming more than 10% of the total nannoplankton assemblage. These major taxa are *C. pelagicus*, *R. minuta*, and *R. haqii* (Fig. 9). Other *Coccolithus* species, such as *C. miopelagicus*, are rare in the investigated samples. The minor taxa were present at low to moderate abundance and ranged from less than 1 to 5% in the samples. They include the genera *Helicosphaera*, *Pontosphaera*, and *Sphenolithus*, as well as *Calcidiscus leptoporus*, *B. bigelowii*, *Microantholithus vesper*, and some species from *Reticulofenestra* such as *R. perplexa*. Most of these taxa show no continuity throughout the studied section.

The species richness and diversity in the studied section are considered low to moderate (Fig. 8). Species richness (S) varies from 3 to 20 species per sample. Samples B11, B37, B40, and B85 have the most taxa (ranging from 18 to 20), while samples B55 and B31 have the fewest (only three taxa). It is observed that the species richness is generally higher in the lower and middle parts of the Nukhul Formation than in its upper part. It is also increased in the lower part of the Rudies Formation. The Shannon-Wiener diversity index ranges from 0.4506 to 1.704. It is noted that the Shannon index decreases in the first samples (B5-B41) and increases in the middle part of the Nukhul Formation (samples B42-B57). The dominance index in the studied section contains values from 0.22 to 0.78.

Sequence stratigraphy

The study of lithofacies, microfacies, biostratigraphy, and depositional environments resulted in the differentiation of three depositional sequences in the Wadi Baba based on the standard model defined by Catuneanu (2006) and Catuneanu et al. (2009).

First depositional sequence (DS-1)

This sequence falls within NN1 and the lower part of NN2 nannofossil zones of the Aquitanian age (samples B5-B40; Fig. 3). The DS-1 is bounded at the base by SB 1 (Fig. 2a) and can be marked by 5 m of polymictic conglomerates at the contact between the Darat and Nukhul formations. The thickness of the sequence is approximately 30 m. The conglomerate layer and the overlying sublithic arenite with reworked foraminiferal tests represent the low stand system tract (LST) which directly overlies the SB 1 in the first depositional sequence. The transgressive surface is located within the lithological boundary between sandstone and marl lithofacies. The retrogradational transgressive system tract (TST) is characterised by a succession of sandy limestone of shoal/tidal flat setting, marl of proximal open marine setting, overlain by mudstone of distal open marine setting (Fig. 2d). The maximum flooding surface (MFS) has occurred at the top of the mudrocks of an open marine setting, which is considered the deepest facies in the studied section (Fig. 2e). The high stand (HST) stacking pattern is composed of alterations of sandy limestone (sandy oyster rudstone and sandy bivalve grain-rudstone microfacies) of shoals and sandstone lithofacies (sublithic arenite petrofacies) of tidal flats (Fig. 2d). The Shannon index ranges from 0.036 to 1.062 in this interval. It is remarked that the species richness decreases within the latest samples of the interval (from 11 in sample B5 to 2 in sample B40). The abundance of the cool nutrient-rich water *R. minuta* increases from up to 10% in the basal Aquitanian to 27% in the upper part of the Aquitanian, indicating more proximity to the shoreline and a falling sea level curve at the end of the Aquitanian. All these data indicate low sea level during the basal Aquitanian age, coupled with intensive rift tectonic activity.

Second depositional sequence (DS-2)

This depositional sequence falls within the upper part of the calcareous nannofossil Zone NN2 of the Burdigalian age (samples from B 41 to B 68). The DS-2 is bounded at the base by SB-2 (Aquitanian/Burdigalian boundary), which is marked by a hiatus due to the absence of the CNM3 Zone of Backman et al. (2012). It is also associated with an abrupt facies change from sandy limestone to marl lithofacies. Above SB 2, a transgressive system tract (TST) was deposited, and the transgressive surface is matched with the sequence boundary. The TST is characterised by marl and mudrock lithofacies that are deposited in an open marine depositional environment. Alternations of massive sandstone and burrowed sandy limestone (recrystallised grainstone microfacies) deposited at the top of TST indicate a tidal flat/shoal depositional environment (Fig. 2f). These deposits represent the HST stacking pattern. In this sequence, the low-stand system tract is not observed and the TST directly overlies the SB 2. The thickness of this sequence is 29 m. The interval contains the upper part of the Nukhul Formation of

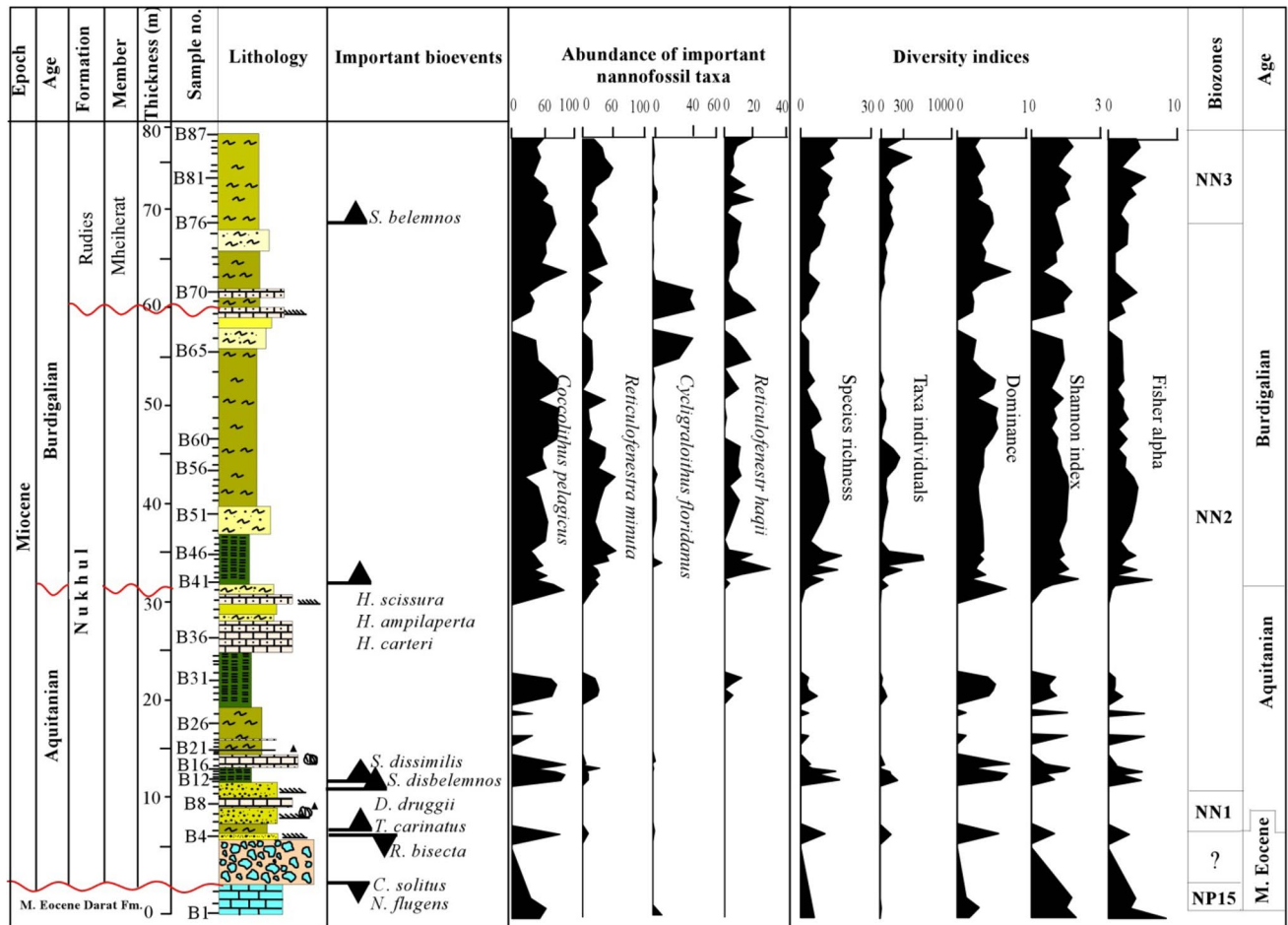


Fig. 9 Important bioevents, the abundance of important nannofossil taxa, diversity indices, and biozonation in the studied section

Burdigalian age. The diversity indices increase in this interval more than in the previous interval (Fig. 9), which indicates high eustatic sea level conditions. As the Shannon index increases from 0.04506 in the latest Aquitanian to 1.893 at the beginning of Burdigalian, in most of the interval, the Shannon index ranges from 1.036 to 1.602. At the last samples of the Nukhul Formation, the decrease in diversity indices indicates a fall in sea level (Fig. 9). From petrographic studies, most of this interval is deposited in an open marine setting environment while at the end of this interval, the presence of a sandy limestone unit may attribute to a shoal depositional environment associated with eustatic sea level falling.

Third depositional sequence (DS-3)

DS-3 formed during the Burdigalian stage above a transgressive surface composite with SB 3. It occurs within the NN2 Zone and the lower part of the NN3 Zone. It is bounded at the base by the facies change from burrowed sandy limestone in the latest sequence 2 to the marl of a deep marine setting. The TST of DS-3 is dominated by marl with intercalations of thin layers

of sandy limestone lithofacies. The thickness of DS-3 is nearly 21 m and is represented by the lowermost part of the Rudies Formation (samples from B 69 to B 87). Palaeontologically, this sequence shows an increase in the abundance and diversity of nannofossils with vertical lithofacies changes, but no hiatus in the nannofossil zones is recorded. Microscopically, it consists of foraminiferal packstone and foraminiferal wacke-mudstone with a higher percentage of planktonic foraminifera, indicating sea level rising and deeper conditions than the upper part of the Nukhul Formation. The diversity increases in this interval concerning the latest samples in the Nukhul Formation (Fig. 9). This indicates the recovery of sea level rise after its falling in the upper part of the Nukhul Formation.

Discussion

Age assignment and important nannofossil bioevents

The age of the early-rift Nukhul Formation in west-central Sinai is controversial as outlined by several previous

works due to a scarcity of index fossils, reworking, facies changes, and different time gaps (El-Heiny and Martini 1981; Evans 1988; Soliman et al. 2012; Hewaidy et al. 2012, 2014; El Atfy et al. 2013). It is commonly dated as Early Miocene (e.g. Souaya 1966; NSSC 1974; Andrawis and Abdel Malik 1981; El-Heiny and Martini 1981; Evans 1988; El-Heiny and Morsi 1992; Ahmed and Pocknall 1994; Phillip et al. 1997; Marzouk 1998, 2009; El-Deeb et al. 2004; Issawi et al. 2009; Faris et al. 2009; Youssef 2011; Soliman et al. 2012). However, it was dated probably as Chattian-Aquitainian in some subsurface wells from the southern part of the Gulf of Suez using palynology (e.g. El Atfy et al. 2013), which extends to Burdigalian age in some locations (Soliman et al. 2012). A similar finding is outlined by Hewaidy et al. (2012, 2014), who assigned the Nukhul Formation in Wadi Baba (of the present work) as the late Oligocene-Early Miocene age based on planktonic foraminifera (*Globigerina ciperensis*) and the presence of the Oligocene calcareous nannofossil NP25 Zone of Martini (1971) at the lowermost part of the formation. The calcareous nannofossil bioevents introduced by these works are not sufficient evidence and reconsidering its accuracy is required, therefore the marine late Oligocene in central Sinai is an illusion that should not be present.

The Aquitanian began at 23.03 Ma, according to the geologic time scale (Gradstein et al. 2012; Gradstein and Ogg 2020). The biohorizon sets employed by Martini (1971) and Okada and Bukry (1980) for delineating the calcareous nannofossil biozones across the Oligocene/Miocene transition are considered to be of limited value (Rio et al. 1990; Backman et al. 2012; Agnini et al. 2014). However, many bioevents can be used to define the Oligocene/Miocene boundary, such as the LO of *Helicosphaera recta* (Rio et al. 1990), the LO of *Sphenolithus ciperensis* (Martini 1971; Raffi et al. 2006; Agnini et al. 2014), and the LO of *Sphenolithus capricornutus* (Steininger et al. 1995). As a result, the absence of these taxa in the studied section, which became extinct at the end of the Oligocene, suggests the absence of marine late Oligocene.

The last occurrence of *Sphenolithus delphix* is another important bioevent that can be used to determine the Oligocene/Miocene boundary (Shackleton et al. 2000; Gradstein et al. 2012; Backman et al. 2012; Agnini et al. 2014; Gennari et al. 2018). Zone CNO6 (*Triquetrorhabdulus carinatus* Partial Range Zone) of Agnini et al. (2014) is defined as the interval from Top *Sphenolithus ciperensis* to Top *Sphenolithus delphix*. It corresponds to upper Zone NP25 and lowermost Zone NN1, as well as Subzone CN1a and lowermost Subzone CN1b of Chattian age. Top *Sphenolithus delphix* forms a distinct biohorizon 30 million years before the Oligocene/Miocene boundary (Agnini et al. 2014). It is worth noting that Bergen et al. (2017) classified *S. delphix* based on total size and apical spine length into small *Sphenolithus* with less than 8 mm

and larger *Sphenolithus* with more than 8 mm. Although the first occurrence of *S. microdelphix* (*S. delphix* with a size less than 8 mm) occurred within the upper part of the NP25 Zone along with *S. delphix* of a size more than 8 mm, it continued into the middle part of the NN2 Zone, whereas the large size of *S. delphix* did not extend to the NN1 Zone (Bergen et al. 2017). The present study recorded *S. microdelphix* (Fig. 6.11, 12) without any existence of *S. delphix* in the lowermost part of the studied section, confirming the occurrence of the upper part of Zone NN1 (Aquitainian) at the base of the Nukhul Formation.

The very essential bioevent which is used as a marker of the lower Miocene is the occurrence of *Discoaster druggii* in the basal part of the Nukhul Formation (FO in sample B 5). *D. druggii* was described as a *Discoaster* of more than 15 µm in size (Bramlette and Wilcoxon 1967). In the last decade, De Kaenal and Villa (2010) differentiated the *D. druggii* into three sizes with different ranges: small size, less than 10 µm (NP26 to NN5); 10 to 15 µm (NN1 to NN5); and more than 15 µm (NN2 to NN3). *D. druggii* with a size of 10 to 15 µm is recognised in sample B 5 whereas the *D. druggii* with a size greater than 15 µm is absent. Therefore, this part of the Nukhul Formation belongs to the upper NN1 Zone of the Lower Miocene, which is supported by the complete absence of *H. recta*, *S. ciperensis*, and *S. capricornutus*.

The lower part of the NN2 Zone is occupied by the interval between samples B 11 and B 40. The assumption of a Lower NN2 Zone of the Aquitanian age for these samples depends on the first appearance of *S. disbelemnus* in sample B 11. According to Gennari et al. (2018), *S. disbelemnus* is present above the Oligocene/Miocene boundary and it also defines CNM2 of Backman et al. (2012). In the present study, *S. disbelemnus* is observed just above the base of *D. druggii* with a size of 10 µm. *Sphenolithus dissimilis* is recorded in the next sample (B12), and this close consequent occurrence with *S. disbelemnus* is another good criterion to prove the presence of the lower part of the NN2 Zone.

According to Bergren et al. (2017), the base of *S. dissimilis* is considered a marker for the Lower Miocene horizon. The large size of *D. druggii*, *H. ampilaperta*, and *H. scissura* first occurred and are recorded in sample B 41, indicating the beginning of the upper part of the NN2 Zone. The first appearance of *H. ampilaperta* is in the upper part of the NN2 Zone at 20.4 Ma. (Raffi et al. 2006), and the first appearance of *H. scissura* is at 20.1 Ma. (Boesiger et al. 2017).

There are also main secondary events that debate and prove the Lower Miocene for the studied samples. Agnini et al. (2014) recorded a high abundance of *Cyclicargolithus abisectus* > 10 µm at the uppermost part of Zone NP25. The sub-zonal boundary CN1a/b is defined at the end acme of *C. abisectus* (Okada and Burky 1980). No *Cyclicargolithus* larger than 10 µm is recorded. The recorded one is less than 10 µm in diameter and represents *C. floridanus*.

A few specimens of *Reticulofenestra bisecta* are recorded from sample B5. The LO of this species was used by Perch-Nielsen (1985) and Berggren et al. (1995) to approximate the NP25/NN1 zonal boundary. Other authors used the LO of this species to approximate the NN1/NN2 zonal boundary (e.g. Holcovà 2001). The last occurrence (top) of this taxon according to Young (1998) is within the NN1 zone (22.82–23.13 Ma, Aquitanian).

In the NN1 and NN2 zones of the present study, there are large numbers of reworked species from the Upper Cretaceous to the middle Eocene. The abundance of the reworked species may reach 90% in some samples. This may make confusion in the biostratigraphic use of some important taxa in this interval, such as *Z. bijugatus*. The base of *Z. bijugatus* started in the Thanetian stage within the NP 9 Zone (Agnini et al. 2007), whereas its last occurrence occurred within the NN1 Zone of the Miocene age (Young 1998). However, the reworking might be caused a much higher stratigraphic level of the LO of this species.

Aquitanian/Burdigalian boundary

Gradstein et al. (2012) suggested two events that mark the Aquitanian/Burdigalian boundary. These events are the FO of *Sphenolithus belemnoides* (19.03 Ma) or *Helicosphaera ampilaperta* (20.43 Ma). Fornaciari and Rio (1996) and Lourens et al. (2004) used the FO of *Helicosphaera ampliaperta* for the delineation of the base of Burdigalian. Berggren et al. (1995) suggested placing the Aquitanian/Burdigalian boundary with the magneto-chron C6An. The first occurrence (base) of *H. ampliaperta* (20.4 Ma) in the Burdigalian Stage is near the base of C6An.1r sub-Magnetochron (Raffi et al. 2006, Fig. 5). In the present study, the base of Burdigalian is placed within the NN2 Zone at FO of *H. ampliaperta* in sample B41 in the Nukhul Formation of Wadi Baba section.

Palaeoecological interpretation

The major identified nannofossil species are related to *Helicosphaera*, *Reticulofenestra*, and *Sphenolithus* taxa. Generally, they are mostly moderate to low, except for a few samples that display high abundance. Their distribution is largely controlled by variations in temperature, nutrient availability, the position of the CCD, and sedimentation rates (Loutit et al. 1988; Gaboardi et al. 1994; De Kaenel and Villa 1996). This sensitivity makes calcareous nannofossils a very important tool for palaeoecological interpretations. They were found to thrive in eutrophic to oligotrophic conditions, tropical to subpolar, with surface water at 200 m depth (Perch-Nielsen 1985; Bown and Young 1998). The summary of the eutrophic and oligotrophic taxa of the studied section is obtained in Figure 10. The reworked Cretaceous and Paleogene taxa are observed with higher abundance in

the lower part of the studied section. Statistical analyses of calcareous nannofossils resulted in three groups with taxa that have distinct palaeoecological preferences (Fig. 8):

Group A includes *Coccolithus pelagicus* and *R. minuta* that consist most of nannofossil assemblages (Figs. 5, 8). Both indicate high primary productivity under eutrophic conditions. The taxon, *C. pelagicus*, is evidence of nutrient-rich water (McIntyre and Bé 1967; Roth 1994; Cacho and Moita 2000) and found in different ranges of temperature (−1.7°C to 15°C) (Okada and McIntyre 1979; Winter et al. 1994) and salinity (26.9–36.0 ‰) (Silva et al. 2008). Generally, *Reticulofenestra* dominates the coastal and shallow marine depositional settings (Okada 1983; Young 1998; Jordan and Winter 2000; Okada 2000). The elevated content of small reticulofenestrids as *Reticulofenestra minuta* which is the most in the studied section is often associated with an increased freshwater impact and terrigenous input during sea-level falls (Haq 1980; Aubry 1992; Flores et al. 1995; Wade and Bown 2006; Auer et al. 2014).

Group B comprises very low abundance taxa (1–5%) and is considered to be warm to temperate water taxa such as *Helicosphaera* (Perch-Nielsen 1985). Despite being rare, *Helicosphaera* is rare and less continuous, but their presence indicates near-shore environments (Krhovsky et al. 1992). *Pontosphaera* is very rare and discontinuous in the studied samples, indicating low salinity and shallow marine conditions (Krhovsky et al. 1992; Nagymarosy and Voronina 1992). *Pontosphaera multipora* is the most dominant of the *Pontosphaera* taxa, preferring shelf areas over open seas (Perch-Nielsen 1985). *Sphenolithus* spp., are detected in the studied samples in rare abundance and indicate warm, well-oxygenated surface water and an open marine environment (Aubry 1992; Fornaciari et al. 1996). **Group C** includes *R. haqii* as well as *C. floridanus*. These species indicate nutrient-rich waters without strong fluctuations in temperature, nutrient availability, and surface water turbulence (Aubry 1992).

The abundance fluctuations in the recorded species reflect small-scale palaeoecological conditions in the studied samples. The increase amount of *C. pelagicus* in the lower part of the Nukhul Formation (Aquitanian) indicates cool-nutrient rich waters (Okada and McIntyre 1979; Winter et al. 1994). Extreme environments (very cold, clear, oligotrophic, and eventually dystrophic) were suggested for some samples from the Ghara Member of the Nukhul Formation by palynological study of El-Atfy et al. (2013) depending on the sporadic occurrence of *Botryococcus* in the absence of other coccal green algae such as *Pediastrum*. The occurrence of *R. minuta* indicates a strong terrigenous influx with raised nutrient availability possibly coupled with an increased stratification of water masses (Ćorić and Hohenegger 2008). The

Genera	Species included	Paleoecological interpretation	Reference
<i>C. pelagicus</i> spp.	<i>C. pelagicus</i> <i>C. miopelagicus</i>	Cool to temperate, eutrophic	4, 6, 7, 8, 9
<i>R. minuta</i>	<3 um	Opportunistic, cool,	14
<i>R. haqii</i>	3-5 um	Warm	5
<i>C. floridanus</i>		Temperate, cosmopolitan	1, 5, 6, 8
<i>Helicosphaera</i> spp.	<i>H. euphratis</i> , <i>H. carteri</i> , <i>H. obliqua</i> , <i>H. ampilaperta</i> <i>H. scissura</i> , <i>H. intermedia</i> and <i>H. mediterranea</i>	Warm to temperate, nearshore eutrophic	2, 6, 10
<i>Discoaster</i> spp.	<i>D. deflandrei</i> , <i>D. druggii</i>	Warm, oligotrophic	3, 6
<i>Pontosphaera</i> spp.	<i>P. multipora</i>	Nearshore	2
<i>Sphenolithus</i> spp.	<i>S. morformis</i> , <i>S. conicus</i> , <i>S. dissimilis</i> , <i>S. microdelphix</i> and <i>S. belemnos</i>	Warm, oligotrophic	4, 5, 6, 7, 9
<i>B. bigelowii</i>		Oligotrophic	11, 12, 13

Fig. 10 Palaeoecological interpretation of the identified nannofossil species in the studied area. 1 Aubry 1992. 2 Perch-Nielsen 1985, 3 Bukry 1973; 4 Haq and Lohmann 1976; 5 Haq 1980; 6 Wei and Wise

1990; 7 Wei and Wise 1992 8 Monechi et al. 2000, 9 Villa and Per-sico 2006 10 Ziveri et al. 2004, 11 Cunha and Shimabukuro 1996; 12 Peleo-Alampay et al. 1999; 13 Svabenicka 1999; 14 Roessig 2007

high amounts of reworked Cretaceous and Palaeogene nanoplankton taxa in the lower part of the Nukhul Formation indicate transportation from the input of surface-bound fresh water as suggested by Auer et al. (2014).

In the middle part of the Nukhul Formation (base of Burdigalian), the *C. pelagicus* became moderate in abundance coupled with moderate to highly moderate abundance of *R. minuta*, (Fig. 9) and a slight increase in warm-taxa such as *Pontosphaera*, *Sphenolithus*, and *Discoaster*. The increase in *R. minuta* was interpreted as indicative of high nutrient levels, influence of terrigenous input, relative proximity to the shore, and points toward warmer conditions. The high abundance of *R. minuta* which indicates an increased fresh-water impact may be coinciding with a sufficiently distinct record of freshwater algae *Pediastrum* and *Botryococcus*,

and the freshwater fern *Magnastriatites howardi* from the Miocene Nukhul Formation by El-Atfy et al. (2013). At the end of the middle part of the Nukhul Formation (within Burdigalian), the increase in abundance of *C. pelagicus* with a lesser amount of *R. minuta* indicates similar conditions to the Aquitanian. The nanoplankton individuals and species richness become very low around the boundary between Nukhul and Rudies formations.

Palaeoenvironmental conditions and sea level-curve

Two third-order depositional sequences with five system tracts recorded in the studied section are related to relative sea level changes and can be correlated with the global sea level curves of Haq et al. (1988); Hardenbol et al. (1998);

and Miller et al. (2005). The two recorded depositional sequences match the third-order cycles 1.4 and 1.5 of Haq et al. (1988). Sequence boundary 1 is marked by a hiatus by many authors in Egypt (e.g. El-Azabi 2004; Farouk and Khalifa 2010; Hewaidy et al. 2012). It correlates globally with the major sequence boundary NAq1 of Hardenbol et al. (1998) and the cycle boundary Mi1 of Miller et al. (2005). Toward the end of the Aquitanian, a significant sea level drop took place, resulting in the deposition of progradational parasequence sets of tidal flat/shoal settings and topped by SB 2. In the present study, small hiatus is recorded due to the absence of nannofossil zone CNM3. This boundary is recorded by Hewaidy et al. (2014) in Wadi Wasit, west-central Sinai, but without hiatus in nannofossil zones. The SB 2 (Aquitanian/Burdigalian) in the study area has a good match with the global sea level curve NBur 1 of Hardenbol et al. (1998). The SB 3 is recorded between the Nukhul and Rudies formations and within the Burdigalian age. It is indicated by the lithofacies change from the burrowed sandy limestone unit that topped the Nukhul Formation and the overlying marl unit. In Egypt, a similar event was recorded between the two formations and also within the Burdigalian stage by El-Heiny and Morsi (1992). Globally, it corresponds to NBur2 (Hardenbol et al. 1998) and Mi1ab (Miller et al. 2005) major sequence boundaries.

In the Arabian Plate, several stratigraphic schemes and conditions of sea level curves have been introduced by many authors (e.g. Sharland et al. 2001; Haq and Qahtani 2005; Simmons et al. 2007; Simmonds and Davies 2018). The Aquitanian–lower Burdigalian depositional sequence is represented by a single second-order depositional sequence bounded at the base by sequence boundary Ng10 (23 Ma) in the Arabian plate and at the top by Ng20 (19 Ma) within the lower Burdigalian age (Sharland et al. 2001). The sequence boundaries Ng10 and Ng20 can be correlated with SB 1 and SB 3 of the present study, but SB 2 cannot be correlated. This may be because Sharland et al. (2001) introduced one 2nd-order depositional sequence, but the present study divides the succession into two third-order depositional sequences. The MFS Ng10 was recognised between open marine carbonates and shallowing-up succession and can be matched with the MFS of DS 2 in the present study.

The relation between the important stratigraphic surfaces and the values of nannofossil diversity in the studied section has been discussed. Generally, the diversity of calcareous nannofossil assemblages decreases with falling sea level due to the decrease in salinity and increase in nutrients and turbidity (Roth 1987, 1989; De Kaenel and Villa 1996; Leckie and Olson 2003; Schlager 2005; Erba 2006). The inferred sea-level curve is based on the palaeoecological application of characteristic calcareous

nannofossil species, their abundance, dominance, and diversity supported by microfacies types and their interpretations (Figs. 3, 9). It is proven that the diversity increases gradually within the upper NN1 and the lower part of the NN2 zones (above SB1) in marl and sandy limestone lithofacies indicating sea level rise. Its value increases above SB 2 (within the upper part of NN2 Zone of Burdigalian) to indicate the rising of sea level again and a retrogradational stacking pattern. It is noticed that the diversity decreases in the uppermost samples of the Nukhul Formation, which indicates sea level falling at the contact between the Nukhul and Rudies formations (SB 3; Fig. 9).

The response of the nannofossil assemblage to the sea-level conditions is observed in the studied samples. The lower Nukhul Formation is characterised by an increase in *C. pelagicus* abundance (up to 83%) and a shortage in *R. minuta* (which ranges from 6 to 10 % in abundance), coupled with a gradual increase in diversity. This result could be positively correlated with a gradual rise in sea level during this interval. An increase in *R. minuta* (19%–52%) and a relative decrease in *C. pelagicus* abundance (30%–55%) are recorded in the basal part of the middle part of the Nukhul Formation. This interval also exhibits an increase in warm water taxa such as *Discoaster*, *Sphenolithus*, and *Helicosphaera*. This assemblage reflects a slight proximity to the shoreline and a temperate condition. It was followed by the continuous sea level rise within the second transgressive phase which is indicated by the low abundance in the content of *R. minuta* again. In the Rudies Formation at the beginning of the Burdigalian, again the *C. pelagicus* increased with a slight decrease in *R. minuta* indicating a slight rise in sea level after the fall in the latest part of the Nukhul Formation.

Conclusion

The present study gives a new outlook on the age assignment of the Nukhul Formation in the outcrops of west-central Sinai (Egypt) using the calcareous nannofossil data. The calcareous nannofossil assemblage and its successive bioevents indicate that the interval of the Nukhul Formation at the studied sections runs from about 21 Ma to 18.9 Ma and includes almost all the Aquitanian with nannofossil zones that belong to upper NN1, lower NN2, and the Burdigalian upper NN2 Zone. The nannofossil taxa in the section show high abundances of both *C. pelagicus* and *R. minuta* and minor species of *C. floridanus*, *Helicosphaera*, *Sphenolithus*, *Discoaster*, and *Pontosphaera*. The study used an important authorization to notice the small fluctuations in the sea level across the section. Cluster analysis was performed and divided the recorded taxa in the studied sample into three assemblages based on their palaeoecological

indications. The data is indicative of nearshore deposits with eutrophic conditions with fresh water influence and terrigenous influx in parts of the section. There is also high nutrient availability with cool to temperate surface water conditions. This allows us to differentiate the studied section into five intervals. The Miocene succession begins with marine sediments with cool nutrient-rich water after the sea level drops between the Eocene and the beginning of the Miocene. The conditions become more influenced by the fresh water and terrigenous input in the middle part of the section as it points to a decrease in water depth. This is proved by the increase of warm taxa as well as a higher percentage of nearshore taxa such as *R. minuta*. The sea level begins to rise again with the beginning of the Burdigalian Stage with a small transgressive phase.

Based on sequence stratigraphic studies, three third-order depositional sequences are recognised with major and minor sequence boundaries that correspond to the middle Eocene/early Aquitanian, Aquitanian/earliest Burdigalian, and within the Burdigalian Stage that match well with the global eustatic sea-level drops.

Appendix

Cited taxa

Braarudosphaera bigelowii (Gran and Braarud, 1935)
Calcidiscus leptoporus (Murray and Blackman, 1898)
 Loeblich and Tappan, 1978
Chiasmolithus bidens (Bramlette and Sullivan, 1961) Hay and Mohler, 1967
Chiasmolithus solitus (Bramlette and Sullivan, 1961) Locker, 1968
Coccolithus miopelagicus (Bukry, 1971)
Coccolithus pelagicus (Wallich, 1877) Schiller, 1930
Coronocyclus nitescens (Kamptner, 1963), Bramlette and Wilcoxon 1967
Cyclicargolithus floridanus Bukry, 1971 (Roth and Hay, in Hay et al., 1967) Bukry, 1971
Discoaster deflandrei Bramlette and Riedel, 1954
Discoaster druggii Bramlette and Wilcoxon, 1967
Helicosphaera ampliapertura Bramlette and Wilcoxon, 1967
Helicosphaera carteri (Wallich, 1877) Kamptner, 1954
Helicosphaera euphratis Haq, 1966
Helicosphaera intermedia Martini, 1965
Helicosphaera leesia da Gama and Varol, 2013
Helicosphaera mediterranea Müller, 1981
Helicosphaera obliqua Bramlette and Wilcoxon, 1967
Helicosphaera scissura Miller, 1981
Helicosphaera truempyi Biolzi and Perch-Nielsen, 1982
Nannotetrina fulgens (Stradner, in Martini and Stradner, 1960) Achuthan and Stradner, 1969

Micrantholithus vesper Deflandre, 1950
Pontosphaera multipora (Kamptner, 1948 ex Deflandre in Deflandre and Fert, 1954) Roth, 1970
Reticulofenestra bisecta (Hay, Mohler and Wade, 1966) Roth, 1973
Reticulofenestra daviesii (Haq, 1968) Haq, 1971
Reticulofenestra dictyoda (Deflandre in Deflandre and Fert, 1954) Stradner in Stradner and Edwards, 1968
Reticulofenestra haqii Backman, 1978
Reticulofenestra lockeri Müller, 1970
Reticulofenestra minuta Roth, 1970
Reticulofenestra perplexa (Burns, 1975) Wise, 1983
Reticulofenestra producta (Kamptner, 1963) Varol, 1989
Sphenolithus belemnos Bramlette and Wilcoxon, 1967
Sphenolithus conicus Bukry, 1971
Sphenolithus disbelemnos Fornaciari and Rio, 1996
Sphenolithus dissimilis Bukry and Percival, 1971
Sphenolithus microdelphix Bergen and de Kaenel, in Bergen et al., 2017
Sphenolithus moriformis (Bronnimann and Stradner, 1960) Bramlette and Wilcoxon, 1967
Thoracosphaera operculata Bramlette and Martini, 1964
Triquetrohabdulus carinatus Martini, 1965
Zygrhablithus bijugatus (Deflandre and Fert, 1954) Deflandre, 1959

Acknowledgements Great thanks to Prof. Dr. Faris, M., Geology Department, Tanta University, Egypt for detailed critical comments and fruitful suggestions of an earlier draft. The authors would like to thank two anonymous reviewers whose careful and perceptive comments greatly improved the paper.

Data Availability Statement The original contributions presented in the study are included in the article; further inquiries can be directed to the corresponding author.

Author Contributions Aziz Abu Shama: Ideas; filed works; checking the results of laboratory investigations, writing and concept of the initial paper, preparation, creation, and presentation of the data.

Sherif Farouk: Ideas; filed works; formulation and evolution of overarching research goals and aims, preparation and writing the initial draft.

Sara El-Nahrawy: filed works; design the idea of the initial paper, preparation, creation, laboratory nannofossil, and microfacies examinations.

Funding Open access funding provided by The Science, Technology & Innovation Funding Authority (STDF) in cooperation with The Egyptian Knowledge Bank (EKB).

Declarations

Conflict of Interest The authors declare that the research was conducted in the absence of any commercial or financial relationships that could be construed as a potential conflict of interest. The authors declare that they have no known competing financial interests or personal relationships that could have appeared to influence the work reported in this paper.

Open Access This article is licensed under a Creative Commons Attribution 4.0 International License, which permits use, sharing, adaptation, distribution and reproduction in any medium or format, as long as you give appropriate credit to the original author(s) and the source, provide a link to the Creative Commons licence, and indicate if changes were made. The images or other third party material in this article are included in the article's Creative Commons licence, unless indicated otherwise in a credit line to the material. If material is not included in the article's Creative Commons licence and your intended use is not permitted by statutory regulation or exceeds the permitted use, you will need to obtain permission directly from the copyright holder. To view a copy of this licence, visit <http://creativecommons.org/licenses/by/4.0/>.

References

- Abul-Nasr, R., & Salama, G. (1999). Paleocology and depositional environments of the Miocene rocks in western Sinai, Egypt. Middle East Research Center, Ain Shams University, *Earth Science Series*, 13, 92–134.
- Adabi, M. H., Zohdi, A., Ghabeishavi, A., & Amiri-Bakhtiyar, H. (2008). Applications of nummulitids and other larger benthic foraminifera in depositional environment and sequence stratigraphy: an example from the Eocene deposits in Zagros Basin, SW Iran. *Facies*, 54(4), 499–512.
- Agnini, C., Fornaciari, E., Raffi, I., Rio, D., Röhl, U., & Westerhold, T. (2007). High-resolution nannofossil biochronology of middle Paleocene to early Eocene at ODP Site 1262: Implications for calcareous nannoplankton evolution. *Marine Micropaleontology*, 64(3–4), 215–248.
- Agnini, C., Fornaciari, E., Raffi, I., Catanzariti, R., Pälke, H., Backman, J., & Rio, D. (2014). Biozonation and biochronology of Paleogene calcareous nannofossils from low and middle latitudes. *Newsletters on Stratigraphy*, 47(2), 131–181.
- Ahmed, A., & Pocknall, D. (1994). The application of palynology to exploration in the Miocene-Pliocene sequence in the Gulf of Suez, Egypt. *Proceedings of the EGPC, Cairo*, 1, 468–481.
- Al-Husseini, M. I. (2012). Late Oligocene–early Miocene nukhul sequence, Gulf of Suez and Red Sea. *GeoArabia*, 17(1), 17–44.
- Andrawis, S. F., & Abdelmalik, W. M. (1981). Lower/middle Miocene boundary in Gulf of Suez region, Egypt. *Newsletters on Stratigraphy*, 10, 156–163.
- Aubry, M.P. (1992) Paleogene Calcareous Nannofossils from the Kerguelen Plateau, Leg 120. In S.W. Wise, R. Schlich, et al. (Eds.), *Proceedings of the Ocean Drilling Program, Scientific Results, Ocean Drilling Program, College Station*, 471–491.
- Auer, G., Piller, W. E., & Harzhauser, M. (2014). High-resolution calcareous nannoplankton palaeoecology as a proxy for small-scale environmental changes in the Early Miocene. *Marine Micropaleontology*, 111, 53–65.
- Ayyad, H. M., & Hewaidy, A. G. A. (2016). Chattian-Aquitania calcareous nannofossil biostratigraphy of the Nukhul Formation in Wadi Baba Section, West Central Sinai, Egypt. *Stratigraphy*, 13(1), 67–81.
- Backman, J., Raffi, I., Rio, D., Fornaciari, E., & Pälke, H. (2012). Biozonation and biochronology of Miocene through Pleistocene calcareous nannofossils from low and middle latitudes. *Newsletters on Stratigraphy*, 45(3), 221–244.
- Bassiouni, M. A. A., & Luger, P. (1990). Maastrichtian to early Eocene ostracoda from southern Egypt. *Palaeontology, palaeoecology, palaeobiogeography and biostratigraphy. Berliner geowissenschaftliche. Abhandlungen, Reihe A*, 120, 755–928.
- Bergin, J., de Kaenel, E., Blair, S., Boesiger, T., & Browning, E. (2017). Oligocene-Pliocene taxonomy and stratigraphy of the genus *Sphenolithus* in the circum North Atlantic Basin: Gulf of Mexico and ODP Leg 154. *Journal of nannoplankton research*, 37(2–3), 77–112.
- Berggren, W. A., Kent, D. V., Swisher, C. C., & Aubry, M. P. (1995). A Revised Cenozoic Geochronology and Chronostratigraphy. In W. A. Berggren, D. V. Kent, M. P. Aubry, & J. Hardenbol (Eds.), *Geochronology, Time Scales and Global Stratigraphic Correlation, Special Publication of Society for Sedimentary Geology, Tulsa*, 54, 129–212.
- Blair, T.C., & McPherson, J.G., (1994). Alluvial fan processes and forms (pp. 354–402). In A. D. Abrahams, & A. J. Parson (Eds.), *Geomorphology of Desert Environments*, London: Chapman & Hall.
- Boesiger, T., De Kaenel, E., Bergin, J., Browning, E., & Blair, S. (2017). Oligocene to Pleistocene taxonomy and stratigraphy of the genus *Helicosphaera* and other placolith taxa in the circum North Atlantic Basin. *Journal of nannoplankton research*, 37(2–3), 145–175.
- Bosworth, W., & McClay, K. (2001). Structural and stratigraphic evolution of the Gulf of Suez rift, Egypt: a synthesis. *Mémoires du Muséum national d'histoire naturelle (1993)*, 186, 567–606.
- Bown, P.R., & Young, J.R., (1998). Techniques. In P. R. Bown (Ed.), *Calcareous Nannofossil Biostratigraphy* (pp. 16–28). London: Kluwer Academic.
- Bramlette, M., & Wilcoxon, J. (1967). Middle Tertiary calcareous nannoplankton of the Ciperio section, Trinidad, WI. *Tulane Studies in Geology and Paleontology*, 5(3), 1–131.
- Bukry, D. (1973). Low latitude coccolith biostratigraphic zonation. *Deep Sea Drilling Project Initial Reports*, 15, 685–703.
- Burchette, T. P., & Wright, V. P. (1992). Carbonate ramp depositional systems. *Sedimentary geology*, 79(1–4), 3–57.
- Cachão, M., & Moita, M. (2000). Coccolithus pelagicus, a productivity proxy related to moderate fronts off Western Iberia. *Marine Micropaleontology*, 39(1–4), 131–155.
- Carr, I. D., Gawthorpe, R. L., Jackson, C. A., Sharp, I. R., & Sadek, A. (2003). Sedimentology and sequence stratigraphy of early syn-rift tidal sediments: the Nukhul Formation, Suez Rift, Egypt. *Journal of sedimentary research*, 73(3), 407–420.
- Catuneanu, O. (2006). *Principles of sequence stratigraphy* (pp. 1–375). Amsterdam: Elsevier.
- Catuneanu, O., Abreu, V., Bhattacharya, J.P., Blum, M.D., Dalrymple, R.W., Eriksson, P.G., Fielding, C.R., Fisher, W.L., Galloway, W.E., Gibling, M.R., Giles, K.A., Holbrook, J.M., Jordan, R., Kendall, C.G. St. C., Macurda, B., Martinsen, O.J., Miall, A.D., Neal, J.E., Nummedal, D., Pomar, L., Posamentier, H.W., Pratt, B.R., Sarg, J.F., Shanley, K.W., Steel, R.J., Strasser, A., Tucker, M.E., & Winker, C. (2009). Towards the standardization of sequence stratigraphy. *Earth-Science Reviews* 92, 1–33.
- Čorić, S., Hohenegger, J. (2008). Quantitative analyses of calcareous nannoplankton assemblages from the Baden-Soos section (Middle Miocene of Vienna Basin, Austria). *Geologica Carpathica*, 59(5), 447–460.
- Colletta, B. P. L. Q., Le Quellec, P., Letouzey, J., & Moretti, I. (1988). Longitudinal evolution of the Suez rift structure (Egypt). *Tectonophysics*, 153(1–4), 221–233.
- Cunha, A., & Shimabukuro, S. (1996). Evidence of Braarudoshaera bloom at the Cenomanian-Turonian boundary of the Santos Basin, Brazil. *IGCP Project*, 381, 17–18.
- De Kaenel, E., & Villa, G. (1996) Oligocene-Miocene calcareous nannofossil biostratigraphy and paleoecology from the Iberia Abyssal Plain. In R. B. Whitmarsh, D. S. Sawyer, A. Klaus, D. G. Masson (Eds.), *Proceedings of the Ocean Drilling Program, Scientific Results, Ocean Drilling Program 149, College Station, TX (Ocean Drilling Program)*, 79–145.
- De Kaenel, E., & Villa, G. (2010). Nannofossil definition of the Oligocene/Miocene boundary at Lemme-Carrosio stratotype (Italy). *International Nannoplankton Association* 13, 5–10.

- Dunham, R. J. (1962). Classification of Carbonate Rocks According to Depositional Texture. In W. E. Ham (Ed.), *Classification of Carbonate Rocks*, American Association of Petroleum Geologists, Tulsa, 108–121.
- EGPC “Egyptian General Petroleum Corporation”, (1964). Oligocene and Miocene rock-stratigraphy of the Gulf of Suez region. *Unpublished report of the Stratigraphic Committee*, 1–142.
- El-Azabi, M. (1997). The Miocene marginal marine facies and their equivalent deeper marine sediments in the Gulf of Suez, Egypt, a revised stratigraphic setting, *Egyptian Journal of Geology*, *41*, 273–308.
- El-Azabi, M. (2004). Facies characteristics, depositional styles and evolution of the Syn-rift Miocene sequences in Nukhul-Feiran area, Sinai side of the Gulf of Suez rift basin, Egypt. *Sedimentology Egypt*, *12*, 69–103.
- El-Deeb, W., Al-Ashwah, A., & Mandur, M. (2004). Planktonic Foraminifera and Calcareous Nannoplankton Biostratigraphy of the Lower and Middle Miocene Sequence in Wadi Gharandal, Southwest Sinai, Egypt. *Egyptian Journal of Petroleum (Print)*, *13*(1), 105–122.
- El-Heiny, I., & Martini, E. (1981). Miocene foraminiferal and calcareous nannoplankton assemblages from the Gulf of Suez region and correlation. *Géologie Méditerranéenne*, *8*(2), 101–108.
- El Atfy, H., Brocke, R., & Uhl, D. (2013). Age and paleoenvironment of the Nukhul Formation, Gulf of Suez, Egypt: Insights from palynology, palynofacies and organic geochemistry. *GeoArabia*, *18*(4), 137–174.
- El-Ayouty, M. K. A. (1990). Petroleum geology. In R. Said (Ed.), *The Geology of Egypt*. Balkema, Rotterdam, 567–599.
- El-Heiny, I. & Morsi, S. (1992): Stratigraphic correlation of Neogene sediments in the eastern Nile Delta and Gulf of Suez, Egypt. *The 11th Exploration International Conference, EGPC*, Cairo, 166–193.
- Erba, E. (2006). The first 150 million years history of calcareous nannoplankton: biosphere–geosphere interactions. *Palaeogeography, Palaeoclimatology, Palaeoecology*, *232*(2–4), 237–250.
- Evans, A. L. (1988). Neogene tectonic and stratigraphic events in the Gulf of Suez rift area, Egypt. *Tectonophysics*, *153*(1–4), 235–247.
- Faris, M., Samir, A., & Shabaan, M. (2009). Calcareous nannofossil biostratigraphy of the lower and middle Miocene sequence in the Gulf of Suez area, Egypt. *The 6th International Conference on the Geology of Africa, Assiut University, Egypt, II*, 17–44.
- Farouk, S., & Khalifa, M. (2010). Facies tracts and sequence development of the Middle Eocene–Middle Miocene successions of the southwestern Qattara Depression, northern Western Desert, Egypt. *Paläontologie, Stratigraphie, Fazies*, *18*(C536), 195–215.
- Fawzy, H. & Abdel Aal, A. (1984). *Regional study of Miocene evaporates and Pliocene-recent sediments in the Gulf of Suez* (pp. 49–74). *The 7th Egyptian General Petroleum Corporation Exploration Seminar, EGPC*, Cairo.
- Flores, J., Sierro, F., & Raffi, I. (1995). Evolution of the calcareous nannofossil assemblage as a response to the paleoceanographic changes in the eastern equatorial Pacific Ocean from 4 to 2 Ma (Leg 138, Sites 849 and 852). In N. G. Pisias, L. A., Mayer, T. R. Janecek, A. Palmer-Julson, & T. H. van Andel (Eds.), *Proceedings of the Ocean Drilling Program, Scientific Results*, *138*.
- Flügel, E. (2004). Carbonate depositional environments (pp. 7–52). In E. Flügel (Ed.), *Microfacies of Carbonate Rocks*. Berlin, Heidelberg: Springer.
- Flügel, E. (2010). Microfacies and archaeology (pp. 903–915). In E. Flügel (Ed.), *Microfacies of carbonate rocks*, Berlin, Heidelberg: Springer.
- Flügel, E., & Munnecke, A. (2010). *Microfacies of carbonate rocks: analysis, interpretation and application* (pp. 1–976), Berlin: Springer.
- Fornaciari, E., & Rio, D. (1996). Latest Oligocene to early middle Miocene quantitative calcareous nannofossil biostratigraphy in the Mediterranean region. *Micropaleontology*, 1–36.
- Fornaciari, E., Di Stefano, A., Rio, D., & Negri, A. (1996). Middle Miocene quantitative calcareous nannofossil biostratigraphy in the Mediterranean region. *Micropaleontology*, 37–63.
- Gaboardi, S., Reale, V., Iaccarino, S., Monechi, S. & Villa, G. (1994). Paleontological response to sea-level change in depositional sequences of the Figols Allogroup between the Isabena and Esera Valleys (pp. 66–76). In E. Mutti, G. Davoli, S. Mora, & M. Sgavetti (Eds.), *The eastern sector of the south-central folded Pyrenean foreland: Criteria for stratigraphic analysis and excursion notes*. Second High-Resolution Sequence Stratigraphy Conference, Tremp, Spain. Instit. Geol., Parma Univ, Italy.
- Gadallah, M. M., S.M. Zaid, & E. Salah Eldin. (2007). Recognition of depositional environments of Nukhul Formation in West central Sinai, Egypt. *Journal of Applied Geophysics*, *6*, 111–124.
- Garfunkel, Z., & Bartov, Y., (1977). The tectonics of the Suez rift. *Israel Geological Survey Bulletin*, *71*, 1–44.
- Geel, T. (2000). Recognition of stratigraphic sequences in carbonate platform and slope deposits: empirical models based on microfacies analysis of Palaeogene deposits in southeastern Spain. *Palaeogeography, Palaeoclimatology, Palaeoecology*, *155*(3–4), 211–238.
- Geisen, M., Bollmann, J., Herrle, J. O., Mutterlose, J., & Young, J. R. (1999). Calibration of the random settling technique for calculation of absolute abundances of calcareous nannoplankton. *Micropaleontology*, *45*(4), 437–442.
- Gennari, R., Persico, D., Turco, E., Villa, G., Iaccarino, S. M., Florindo, F., Lurcock, P. C., & Zerkass, G. (2018). High-resolution integrated calcareous plankton biostratigraphy and magnetostratigraphy at the Oligocene–Miocene transition in southwestern Atlantic Ocean. *Geological Journal*, *53*(3), 1079–1101.
- Gertsch, B., Adatte, T., Keller, G., Tantawy, A. A., Berner, Z., Mort, H. P., & Fleitmann, D. (2010). Middle and late Cenomanian oceanic anoxic events in shallow and deeper shelf environments of western Morocco. *Sedimentology*, *57*(6), 1430–1462.
- Gradstein, F. M., & Ogg, J. G. (2020). The chronostratigraphic scale (pp. 21–32). In *Geologic Time Scale 2020*, Amsterdam: Elsevier.
- Gradstein, F. M., Ogg, J. G., Schmitz, M. B., & Ogg, G. M. (2012). *The geologic time scale 2012* (pp. 1–1176), Amsterdam: Elsevier.
- Hammer, Ø., & Harper, D. (2006). Morphometrics. In *Paleontological Data Analysis* (pp. 78–156). Oxford: Blackwell Publishing.
- Hammer, Ø., Harper, D. A., & Ryan, P. D. (2001). PAST: Paleontological statistics software package for education and data analysis. *Palaeontologia electronica*, *4*(1), 9.
- Haq, B. U. (1980). Biogeographic history of Miocene calcareous nannoplankton and paleoceanography of the Atlantic Ocean. *Micropaleontology*, 414–443.
- Haq, B. U., & Lohmann, G. P. (1976). Early Cenozoic calcareous nannoplankton biogeography of the Atlantic Ocean. *Marine Micropaleontology*, *1*, 119–194.
- Haq, B. U., & Al-Qahtani, A. M. (2005). Phanerozoic cycles of sea-level change on the Arabian Platform. *GeoArabia*, *10*(2), 127–160.
- Haq, B. U., Hardenbol, J., & Vail, P. R. (1988). Mesozoic and Cenozoic chronostratigraphy and cycles of sea-level change. In C. K. Wilgus, B. S. Hastings, C.G.St.C. Kendall et al. (Eds.), *Sea-Level Changes: An Integrated Approach, Special Publication of Society for Sedimentary Geology*, *42*, Tulsa, 7–108.
- Hardenbol, J., Thierry, J., Farley, M. B., Jacquin, T., De Graciansky, P.-C., & Vail, P. R. (1998). Mesozoic and Cenozoic sequence chronostratigraphic framework of European basins. *Special Publication of Society for Sedimentary Geology*, *60*, 3–13.
- Hewaidy, A. G. A., Farouk, S., & Ayyad, H. M. (2012). Nukhul Formation in Wadi Baba, southwest Sinai Peninsula, Egypt. *GeoArabia*, *17*(1), 103–120.

- Hewaidy, A. G. A., Farouk, S., & Ayyad, H. M. (2014). Integrated biostratigraphy of the upper Oligocene–middle Miocene successions in west central Sinai, Egypt. *Journal of African Earth Sciences*, *100*, 379–400.
- Hewaidy, A. G. A., Mandur, M. M., Farouk, S., & El Agroudy, I. S. (2016). Integrated planktonic stratigraphy and paleoenvironments of the Lower-Middle Miocene successions in the central and southern parts of the Gulf of Suez, Egypt. *Arabian Journal of Geosciences*, *9*(2), 1–32.
- Holcová, K. (2001). New methods in foraminiferal and calcareous nannoplankton analysis and evolution of Oligocene and Miocene basins of the Southern Slovakia. *Slovak Geological Magazine*, *7*(1), 19–41.
- Hottinger, L. (1983). Processes determining the distribution of larger foraminifera in space and time. *Utrecht Micropaleontological Bulletin*, *30*, 239–253.
- Hottinger, L. (1997). Shallow benthic foraminiferal assemblages as signals for depth of their deposition and their limitations. *Bulletin de la Société géologique de France*, *168*(4), 491–505.
- Hughes, G. W., Abdine, S., & Girgis, M. (1992). Miocene biofacies development and geological history of the Gulf of Suez, Egypt. *Marine and Petroleum Geology*, *9*(1), 2–28.
- Issawi, B., Francis, M., Youssef, A., & Osman, R. (2009). *The Phanerozoic of Egypt: a geodynamic approach* (pp. 1–589). Cairo: Geological Survey of Egypt.
- Jackson, C., Gawthorpe, R., & Sharp, I. (2006). Style and sequence of deformation during extensional fault-propagation folding: examples from the Hammam Faraun and El-Qaa fault blocks, Suez Rift, Egypt. *Journal of Structural Geology*, *28*(3), 519–535.
- Jordan, R., & Winter, A. (2000). Assemblages of coccolithophorids and other living microplankton off the coast of Puerto Rico during January–May 1995. *Marine Micropaleontology*, *39*(1–4), 113–130.
- Krhovský, J., Adamová, M., Hladíková, J., & Maslowská, H. (1992). Paleoenvironmental changes across the Eocene/Oligocene boundary in the Ždánice and Pouzdřany units (Western Carpathians, Czechoslovakia): the long-term trend and orbitally forced changes in calcareous nannofossil assemblages. *Knihovnička ZPN 14b*, 105–187.
- Leckie, R. M., & Olson, H. C. (2003). Micropaleontologic Proxies for Sea-Level Change and Stratigraphic Discontinuities. *Special Publication of Society for Sedimentary Geology*, *75*, 5–19.
- Lourens, L., Hilgen, F., Shackleton, N. J., Laskar, J., & Wilson, D. (2004). The Neogene Period (pp. 409–440). In F. M. Gradstein, J. G. Ogg, & A. G. Smith (Eds.), *A geologic time scale 2004*, Amsterdam: Elsevier.
- Loutit, T. S., Hardenbol, J., Vail, P. R., & Baum, G. R. (1988). Condensed sections: the key to age determination and correlation of continental margin sequences. In C. K. Wilgus, B. S. Hastings, C.G.St.C. Kendall, et al. (Eds.), *Sea-Level Changes: An Integrated Approach. Special Publication of Society for Sedimentary Geology*, *42*, Tulsa, 183–213.
- Lowe, D. R. (1982). Sediment gravity flows; II, Depositional models with special reference to the deposits of high-density turbidity currents. *Journal of sedimentary research*, *52*(1), 279–297.
- Martini, E. (1971). Standard Tertiary and Quaternary calcareous nannoplankton zonation. In A. Farinacci (Ed.), *Proceedings of the Second Planktonic Conference, Roma, 1970*, 739–785.
- Martini, E., & Worsley, T. (1970). Standard Neogene calcareous nannoplankton zonation. *Nature*, *225*(5229), 289–290.
- Marzouk, A. M. (1998). Nannofossil biostratigraphy of the subsurface Miocene section in the Ras Budran Area, Gulf of Suez, Egypt. *Neues Jahrbuch für Geologie und Paläontologie-Abhandlungen*, 19–40.
- Marzouk, A. M. (2009). Nannofossil biostratigraphy of Miocene sections from two wells in the Gulf of Suez, Egypt. *Paläontologie, Stratigraphie, Fazies*, *17*, 101–127.
- McIntyre, A., & Bé, A. W. (1967). Modern coccolithophoridae of the Atlantic Ocean-I. Placoliths and cyrtoliths. *Deep Sea Research, Pergamon Press Ltd. Printed in Great Britain*, *14*, 561–597.
- Miller, K. G., Komins, M. A., Browning, J. V., Wright, J. D., Mountain, G. S., Katz, M. E., Sugarman, P. J., Cramer, B. S., Christie-Blick, N., & Peka, S.F. (2005). The Phanerozoic record of global sea-level change. *Science*, *310*, 1293–1298.
- Monechi, S., Angori, E., & von Salis, K. (2000). Calcareous nannofossil turnover around the Paleocene/Eocene transition at Alamedilla (southern Spain). *Bulletin de la Société géologique de France*, *171*(4), 477–489.
- Moustafa, A. R. (1987). Drape folding in the Baba-Sidri area, eastern side of the Suez rift. *Egyptian Journal of Geology*, *31*, 15–27.
- Moustafa, A. R. (1993). Structural characteristics and tectonic evolution of the east-margin blocks of the Suez rift. *Tectonophysics*, *223*(3–4), 381–399.
- Moustafa, A. R. (1996). Internal structure and deformation of an accommodation zone in the northern part of the Suez rift. *Journal of Structural Geology*, *18*(1), 93–107.
- Moustafa, A. R. (2004). *Geologic maps of the Eastern side of the Suez rift (western Sinai Peninsula), Egypt*. American Association of Petroleum Geologists/Datapages, Inc. GIS Series (Geologic maps and crosssections in digital format on CD).
- Moustafa, A. & Khalil, S. M. (2020). Structural Setting and Tectonic Evolution of the Gulf of Suez, NW Red Sea and Gulf of Aqaba Rift Systems. In Z. Hamimi, A. El-Barkooky, J. M. Frías, H. Fritz, & Y. Abd El-Rahman (Eds.), *The Geology of Egypt* (pp. 295–342), Wiesbaden: Springer.
- Mulder, T., & Alexander, J. (2001). The physical character of subaqueous sedimentary density flows and their deposits. *Sedimentology*, *48*(2), 269–299.
- Nagymarosy A. & Voronina A.A. (1992). Calcareous nannoplankton from the Lower Maykopian Beds (Early Oligocene, Union of Independent States). *Proceeding of the 4th International Nannoplankton Association Conference, Prague. Knihovnička ZPN, 14b* (pp. 189–221). Hodonín: MND - Oil and Gas Company.
- Nemec, W., & Steel, R. (1984). Alluvial and Coastal Conglomerates: Their Significant Features and Some Comments on Gravelly Mass-Flow Deposits. In E. H. Koster, & R. J. Steel, (Eds.), *Sedimentology of Gravels and Conglomerates. Canadian Society of Petroleum Geologists Memoir 10*, 1–31.
- NSSC “National Stratigraphic Subcommittee” (1974). Miocene rock stratigraphy in the Gulf of Suez region. *Egyptian Journal Geology*, *18*, 1–59.
- Okada, H. (1983). Modern nannofossil assemblages in sediments of coastal and marginal seas along the western Pacific Ocean. *Utrecht Micropaleontological Bulletin*, *30*, 171–187.
- Okada, H. (2000). An improved filtering technique for calculation of calcareous nannofossil accumulation rates. *Journal of nannoplankton research*, *22*(3), 203–204.
- Okada, H., & Bukry, D. (1980). Supplementary modification and introduction of code number to the low-latitude coccolith biostratigraphic zonation. *Marine Micropalaeontology*, *5*, 321–325.
- Okada, H., & McIntyre, A. (1979). Seasonal distribution of modern coccolithophores in the western North Atlantic Ocean. *Marine Biology*, *54*(4), 319–328.
- Patton, T., Moustafa, A., Nelson, R., & Abdine, S. (1994). Tectonic evolution and structural setting of the Suez Rift. In S. M. Landon (Ed.), *Interior Rift Basins. American Association of Petroleum Geologists Memoir 59*, 9–55.
- Peijs J.A.M.M., Bevan, T.G., Piombino, J.T. (2012). The Gulf of Suez rift basin. In D. G. Roberts, & A. W Bally (Eds.), *Regional Geology and Tectonics: Phanerozoic Rift Systems and Sedimentary Basin* (pp. 164–194), Amsterdam: Elsevier.
- Peleo-Alampay, A., Mead, G., & Wei, W. (1999). Unusual Oligocene Braarudosphaera-rich layers of the South Atlantic and their

- palaeoceanographic implications. *Journal of nanoplankton research*, 21(1), 17–26.
- Perch-Nielsen, K. (1985) Cenozoic Calcareous Nannofossils. In H. M. Bolli, J. B. Sanders & K. Perch-Nielsen (Eds.), *Plankton Stratigraphy* (pp. 427–554), Cambridge: Cambridge University Press.
- Pettijohn, F. J., Potter, P. E., & Siever, R. (2012). *Sand and sandstone* (pp. 1–631). Heidelberg: Springer Science & Business Media.
- Phillip, G., Imam, M., & Gawad, G. A. (1997). Planktonic foraminiferal biostratigraphy of the Miocene sequence in the area between Wadi El-Tayiba and Wadi Sidri, west central Sinai, Egypt. *Journal of African Earth Sciences*, 25(3), 435–451.
- Pomar, L., Mateu-Vicens, G., Morsilli, M., & Brandano, M. (2014). Carbonate ramp evolution during the late Oligocene (Chattian), Salento Peninsula, southern Italy. *Palaeogeography, Palaeoclimatology, Palaeoecology*, 404, 109–132.
- Popov, S.V., Rögl, F., Rozanov, A.Y., Steininger, F.F., Shcherba, I.G. and Kováč, M. Eds., 2004. Lithological-paleogeographic maps of Paratethys. 10 Maps Late Eocene to Pliocene. *Courier Forschungsinstitut Senckenberg*, 250, 1–46.
- Postma, G. (1984). Mass-flow conglomerates in a submarine canyon: Abrijoja fan-delta, Pliocene, southeast Spain. In E. H. Koster, & R. J. Steel (Eds.), *Sedimentology of Gravels and Conglomerates. Canadian Society of Petroleum Geologists Memoir*, 10, 237–258.
- Raffi, I., Backman, J., Fornaciari, E., Pálíke, H., Rio, D., Lourens, L., & Hilgen, F. (2006). A review of calcareous nannofossil astrochronology encompassing the past 25 million years. *Quaternary Science Reviews*, 25(23–24), 3113–3137.
- Richardson, M., & Arthur, M. A. (1988). The Gulf of Suez-northern Red Sea neogene rift: a quantitative basin analysis. *Marine and Petroleum Geology*, 5(3), 247–270.
- Rio, D., Raffi, I., & Villa, G. (1990). Pliocene-Pleistocene calcareous nannofossil distribution patterns in the Western Mediterranean. *Proceedings of the ocean drilling Program, Scientific Results*, 107, 513–533.
- Robson, D. A. (1971). The structure of the Gulf of Suez (Clysmic) rift, with special reference to the eastern side. *Journal of the Geological Society*, 127(3), 247–271.
- Roessig, K. L. M. (2007). *Miocene climate transitions in the south-west Pacific, Tasmania: Interpretations based on calcareous nannofossils* (pp. 1–320). A dissertation submitted to the Department of Geological Sciences in partial fulfillment of the requirements for the degree of Doctor of Philosophy, College of Arts and Sciences, Tallahassee: Florida State University.
- Rohais, S., Barrois, A., Colletta, B., & Moretti, I. (2016). Pre-salt to salt stratigraphic architecture in a rift basin: insights from a basin-scale study of the Gulf of Suez (Egypt). *Arabian Journal of Geosciences*, 9(4), 1–24.
- Romero, J., Caus, E., & Rosell, J. (2002). A model for the palaeoenvironmental distribution of larger foraminifera based on late Middle Eocene deposits on the margin of the South Pyrenean basin (NE Spain). *Palaeogeography, Palaeoclimatology, Palaeoecology*, 179(1–2), 43–56.
- Roth, P. H. (1987). Mesozoic calcareous nannofossil evolution: relation to paleoceanographic events. *Paleoceanography*, 2(6), 601–611.
- Roth, P. H. (1989). Ocean circulation and calcareous nanoplankton evolution during the Jurassic and Cretaceous. *Palaeogeography, Palaeoclimatology, Palaeoecology*, 74(1–2), 111–126.
- Roth, P. H. (1994). Distribution of coccolith in oceanic sediments. In A. Winter, & W. G., Siesser (Eds.), *Coccolithophores*, 199–218.
- Saoudi A., Khalil, B. (1986). Distribution and hydrocarbon potential of Nukhul sediments in the Gulf of Suez (pp. 75–96). In *Proceedings of the 7th exploration seminar, 1*. Cairo: Egyptian General Petroleum Corporation.
- Schlager, W. (2005). *Carbonate sedimentology and sequence stratigraphy* (pp. 1–200). Society for Sedimentary Geology, Concepts in Sedimentology and Paleontology, 8.
- Scholle, P. A., & Ulmer-Scholle, D. S. (2003). A color guide to the petrography of carbonate rocks: grains, textures, porosity, diagenesis. *American Association of Petroleum Geologists Memoir* 7, 1–474.
- Schütz, K. I. (1994). Structure and Stratigraphy of the Gulf of Suez, Egypt. In S. M. Landon (Ed.), *Interior Rift Basin. American Association of Petroleum Geologists, Memoir*, 59, 57–95.
- Scott, R. W., Govean, F. M. (1985). Early depositional history of a rift basin: Miocene in western Sinai. *Palaeogeography, Palaeoclimatology, Palaeoecology*, 62, 143–158.
- Shackleton, N. J., Hall, M. A., Raffi, I., Tauxe, L., & Zachos, J. (2000). Astronomical calibration age for the Oligocene-Miocene boundary. *Geology*, 28(5), 447–450.
- Sharland, P. R., Archer, R., Casey, D. M., Davies, R. B., Hall, S. H., Heward, A. P., Horbury, A. D & Simmons, M. D. (2001). *Arabian plate sequence stratigraphy* (pp. 1–374). GeoArabia Special Publication, Bahrain: Gulf Petrolink, 2.
- Sharp, I. R., Gawthorpe, R. L., Underhill, J. R., & Gupta, S. (2000). Fault-propagation folding in extensional settings: Examples of structural style and synrift sedimentary response from the Suez rift, Sinai, Egypt. *Geological Society of America Bulletin*, 112(12), 1877–1899.
- Silva, A., Palma, S., & Moita, M. (2008). Coccolithophores in the upwelling waters of Portugal: Four years of weekly distribution in Lisbon bay. *Continental Shelf Research*, 28(18), 2601–2613.
- Simmons, M., & Davies, R. (2018). Triassic to Middle Jurassic stratigraphy of the Arabian Plate: an introduction. In M. C. Poppelreiter (Ed.), *Lower Triassic to Middle Jurassic Sequence of the Arabian Plate*, 9–32.
- Simmons, M. D., Sharland, P. R., Casey, D. M., Davies, R. B., & Sutcliffe, O. E. (2007). Arabian Plate sequence stratigraphy: Potential implications for global chronostratigraphy. *GeoArabia*, 12(4), 101–130.
- Soliman, A., Ćorić, S., Head, M. J., Piller, W. E., & El Beialy, S. Y. (2012). Lower and Middle Miocene biostratigraphy, Gulf of Suez, Egypt based on dinoflagellate cysts and calcareous nannofossils. *Palynology*, 36(1), 38–79.
- Souaya, F. J. (1966). Miocene foraminifera of the Gulf of Suez region, U.A.R.: part 3, Biostratigraphy. *Micropaleontology*, 12(2), 183–202.
- Steininger, F., Aubry, M., Biolzi, M., Borsetti, A., Cati, F., Corfield, R., Gelati, R., Iaccarino, S., Napoleone, C., Rögl, R., Rötzel, R., Spezzaferri, S., Tateo, F., Villa, G., Zevenboom, D. (1995). Chapter A9 Proposal for the global stratotype section and point (GSSP) for the base of the Neogene (the Palaeogene/Neogene Boundary). *Developments in Palaeontology and Stratigraphy*, 15, 125–147.
- Švábenická, L. (1999). Braarudosphaera-rich sediments in the Turonian of the Bohemian Cretaceous Basin, Czech Republic. *Cretaceous Research*, 20(6), 773–782.
- Temraz, M., & Dypvik, H. (2018). The lower Miocene Nukhul Formation (Gulf of Suez, Egypt): microfacies and reservoir characteristics. *Journal of Petroleum Exploration and Production Technology*, 8(1), 85–98.
- Tucker, M. E., & Wright, V. P. (2009). *Carbonate sedimentology* (pp. 1–482). London: John Wiley & Sons, Blackwell Scientific.
- Villa, G., & Persico, D. (2006). Late Oligocene climatic changes: evidence from calcareous nannofossils at Kerguelen Plateau Site 748 (Southern Ocean). *Palaeogeography, Palaeoclimatology, Palaeoecology*, 231(1–2), 110–119.
- Wade, B. S., & Bown, P. R. (2006). Calcareous nannofossils in extreme environments: the Messinian salinity crisis, Polemi Basin, Cyprus. *Palaeogeography, Palaeoclimatology, Palaeoecology*, 233(3–4), 271–286.

- Waite, S.T., Pooley, R.W., 1953. *Report on the Nukhul Formation*. Egyptian General Petroleum Company, unpublished internal report (G.R. 422).
- Wei, W., & Wise Jr, S. W. (1990). Biogeographic gradients of middle Eocene-Oligocene calcareous nannoplankton in the South Atlantic Ocean. *Palaeogeography, Palaeoclimatology, Palaeoecology*, 79(1-2), 29-61.
- Wei, W., & Wise Jr, S. W. (1992). Eocene-Oligocene calcareous nannofossil magnetobiochronology of the Southern Ocean. *Newsletters on Stratigraphy*, 26 (2-3), 119-132.
- Wilson, J. L. (1975). The lower Carboniferous Waulsortian facies. In J. L. Wilson (Ed.), *Carbonate facies in geologic history*, Springer, 148-168.
- Winter, A., Jordan R.W., Roth P. (1994). Biogeography of living coccolithophores in ocean waters. In A. Winter, & W. G. Siesser (Eds.), *Coccolithophores* (pp. 161–177). Cambridge: Cambridge University Press.
- Young, J. R. (1998). Neogene nannofossils. *Calcareous Nannofossil Biostratigraphy* (225, 265). Dordrecht: Kluwer Academic.
- Youssef, A. (2011). Early-Middle Miocene Suez syn-rift-basin, Egypt: A sequence stratigraphy framework. *GeoArabia*, 16(1), 113-134.
- Zalat, A. A. (2018). Palaeoenvironmental reconstruction of the early to Middle Miocene sequence in West Central Sinai, Egypt, as revealed from fossil diatoms. *Acta Geologica Sinica-English Edition*, 92(1), 354-366.
- Ziveri, P., Baumann, K.-H., Böckel, B., Bollmann, J., & Young, J. R. (2004). Biogeography of selected Holocene coccoliths in the Atlantic Ocean. In H. R. Thierstein, & J. R. Young (Eds.), *Coccolithophores*, Springer, 403-428.

Publisher's note Springer Nature remains neutral with regard to jurisdictional claims in published maps and institutional affiliations.